Electronic Supplementary Material (ESI) for Chemical Science.
This journal is © The Royal Society of Chemistry 2018

Electronic Supplementary Information for

Near Infrared Excitation and Emission in Rare Earth MOFs via Encapsulation of Organic Dyes

Chong Liu,[1] Svetlana V. Eliseeva,[2] Tian-Yi Luo,[1] Patrick F. Muldoon,[1] Stéphane Petoud*[2] and Nathaniel L. Rosi*[1]

1. Department of Chemistry, University of Pittsburgh, 219 Parkman Ave., Pittsburgh, PA 15260, United States.

2. Centre de Biophysique Moléculaire, CNRS UPR 4301, 45071 Orléans, France

Contents:

1. General procedures

All purchased chemicals were used without further purification except where otherwise noted. All N,N-dimethylformamide (DMF) used for washing crystals was pre-dried over 4Å molecular sieves.

X-ray powder diffraction patterns were collected using a Bruker AXS D8 Discover powder diffractometer at 40 kV, 40 mA for Cu Kα, (λ = 1.5406 Å) with a scan speed of 0.10 sec/step from 3º to 45º at a step size of 0.02º. The data were analyzed using the EVA program from the Bruker Powder Analysis Software package. The simulated powder patterns were calculated using Materials Studio based on single crystal diffraction data of corresponding MOFs.

Single crystal X-ray diffraction experiments were performed on a Bruker X8 Prospector Ultra diffractometer equipped with an Apex II CCD detector and an IµS micro-focus CuKα X-ray source (λ = 1.54178 Å). Samples were mounted using two different methods: i) a suitable MOF crystal was loaded into a capillary tube which was then flame sealed before mounting. Data were then collected at ambient temperature; ii) a MOF crystal was placed onto MiTeGen MicroMesh using Fluorolube and data were collected under cold N_2 stream at 240 K. SC-XRD data were processed using Bruker APEX II software package.

^{1}H NMR spectra were obtained using a Bruker Avance III 500 MHz spectrometer. Chemical shifts are in parts per million using the residual solvent peak (DMSO-d_6) as the reference value.

N_2 adsorption experiment was performed on a Quantachrome Autosorb-1 instrument at 77 K. Activation procedures are described in detail in 2.11.

Optical microscopic images were obtained using an Olympus BH-2 microscope.

Thermogravimetric analyses (TGA) were performed using a TA Q500 thermal analysis system. All TGA experiments were performed under a N_2 atmosphere from about 20 °C to 600 °C at a rate of 5 °C /min. Data were analyzed using the TA Universal Analysis software package.

The CHN elemental analyses (EA) were performed by the University of Illinois, Department of Chemistry Microanalysis Laboratory using an Exeter Analytical CE440.

Emission, excitation spectra for the **Yb^{3+}-BPDC** and **LDS 750@Yb^{3+}-BPDC** MOF were performed in an integration sphere using samples (2-5 % solids ground with MgO) placed into quartz tubes on the FluoroLog 3 spectrofluorimeter (Horiba Scientific) equipped with a visible photomultiplier tube (PMT) (220-800 nm, R928P; Hamamatsu), and a NIR PMT (950-1650 nm, H10330-75; Hamamatsu). All spectra were corrected for the instrumental functions. Emission signal was selected using iHR-320 monochromator, detected using NIR PMT, fed into a 500 MHz bandpass digital oscilloscope (TDS 754C; Tektronix), transferred to a PC where the data were processed with the Origin 8® program.

2. Syntheses and characterization of MOFs

The protocols in sub-sections 2.1-2.3 to synthesize corresponding MOFs were optimized to balance crystal size, yield, quality and reaction time. Generally, 40 equivalents (based on the MCl_3 used) of the structural directing agent (2,6-difluorobenzoic acid, DFBA) was used. When less DFBA was used, the product crystallized more quickly, with occasional formation of impurities of other unidentified MOFs; when more DFBA was used, the product crystallized more slowly, with increased crystal dimensions. DMF was the sole solvent for NDC and BPDC MOFs. A mixture of DMF/DMA (DMA = *N*,*N*-dimethylacetamide) was used for synthesizing ABDC MOFs, different ratios of the two solvents were tested. Generally, more DMA would yield larger crystals in smaller quantity (slower crystallization). When other salts (such as $M(NO_3)_3 \cdot xH_2O$, $M(OAc)_3 \cdot xH_2O$) were attempted under the same condition to replace $MCl_3 \cdot 6H_2O$, in the presence of DFBA, they did not yield pure phase **fcu** MOFs, but the preparation involving those salts was not fully optimized.

2.1 Synthesis of rare earth-NDC MOFs

Clear stock solutions of H_2-NDC (0.05 M) and $MCl_3 \cdot 6H_2O$ (0.1 M, M = Y^{3+}, Eu^{3+}, Gd^{3+}, Tb^{3+}, Dy^{3+}, Ho^{3+}, Er^{3+}, Tm^{3+}, Yb^{3+}, Lu^{3+}) were prepared by dissolving corresponding compounds in DMF with the aid of ultrasonication. In a 20-mL glass vial, H_2-NDC (0.05 M, 4 mL, 2×10^{-4} mol), $MCl_3 \cdot 6H_2O$ (0.1 M, 1 mL, 1×10^{-4} mol), and DFBA (632 mg, 4×10^{-3} mol) were mixed and briefly sonicated to dissolve DFBA. The vial was tightly capped and heated in a 120 ^{o}C isothermal oven for 24 hours. After cooling to room temperature, the crystals were collected and washed with dry DMF, hereafter denoted as “as-synthesized” MOFs.

2.2 Synthesis of rare earth-BPDC MOFs

Clear stock solutions of $MCl_3 \cdot 6H_2O$ (0.1 M, M = Y^{3+}, Eu^{3+}, Gd^{3+}, Tb^{3+}, Dy^{3+}, Ho^{3+}, Er^{3+}, Tm^{3+}, Yb^{3+}, Lu^{3+}) were prepared by dissolving corresponding compounds in DMF with the aid of ultrasonication. A stock suspension of H_2-BPDC (0.05 M) was prepared by mixing the ligand with DMF and sonicating for 5 min. In a 20-mL glass vial, H_2-BPDC (0.05 M, 4 mL, 2×10^{-4} mol), $MCl_3 \cdot 6H_2O$ (0.1 M, 0.5 mL, 5×10^{-5} mol), and DFBA (316 mg, 2×10^{-3} mol) were mixed and briefly sonicated to dissolve DFBA. The vial was tightly capped and heated in a 120 °C isothermal oven for 24 hours. After cooling to room temperature, the crystals were collected and washed with dry DMF, hereafter denoted as "as-synthesized" MOFs.

2.3 Synthesis of rare earth-ABDC MOFs

Clear stock solutions of $MCl_3 \cdot 6H_2O$ (0.1 M, M = Y^{3+}, Eu^{3+}, Gd^{3+}, Tb^{3+}, Dy^{3+}, Ho^{3+}, Er^{3+}, Tm^{3+}, Yb^{3+}, Lu^{3+}) were prepared by dissolving corresponding compounds in a mixture of DMA and DMF (v/v = 4:1) with the aid of ultrasonication. A stock suspension of H_2-ABDC (0.05 M) was prepared by adding the ligand into a mixture of DMA and DMF (v/v = 4:1) and sonicating for 5 min. In a 20-mL glass vial, H_2-ABDC (0.05 M, 6 mL, 3×10^{-4} mol), $MCl_3 \cdot 6H_2O$ (0.1 M, 0.5 mL, 5×10^{-5} mol), and DFBA (316 mg, 2×10^{-3} mol) were mixed and briefly sonicated to dissolve DFBA. The vial was tightly capped and heated in a 120 °C isothermal oven for 48 hours. After cooling to room temperature, the crystals were collected and washed with dry DMF, hereafter denoted as "as-synthesized" MOFs.

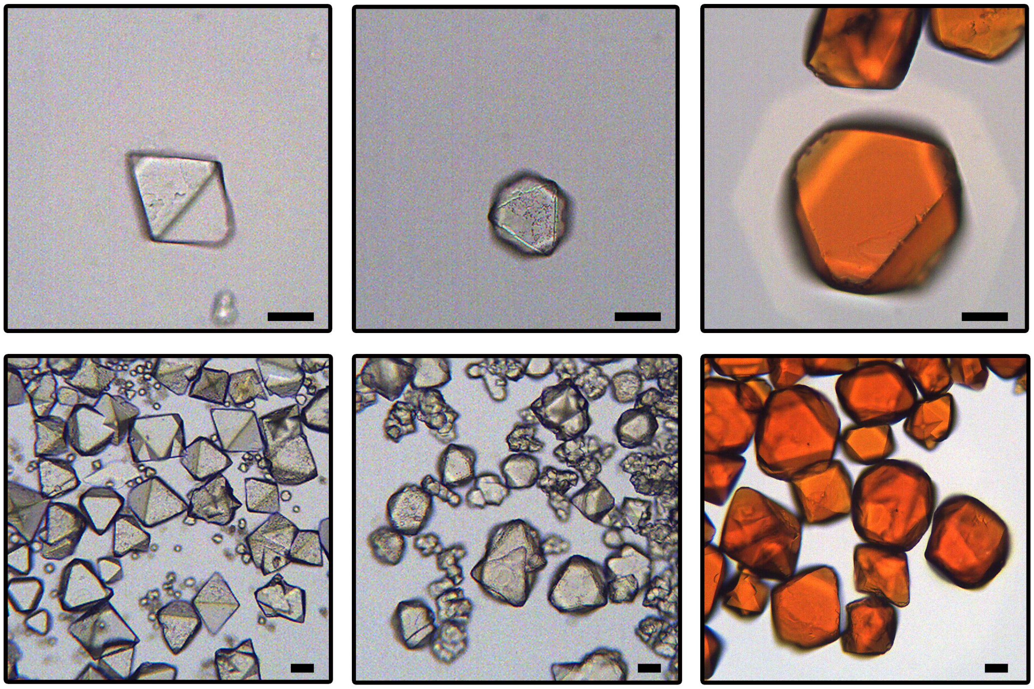

Fig. S1 Optical images of **Dy^{3+}-NDC** (left), **Dy^{3+}-BPDC** (middle), and **Dy^{3+}-ABDC** (right) (all scale bars: 50 μm).

2.4 SC-XRD of Dy^{3+}-NDC MOF

X-ray diffraction data of **Dy^{3+}-NDC** were collected on a Bruker X8 Prospector Ultra equipped with an Apex II CCD detector and an IμS micro-focus CuK\α source (λ = 1.54178 Å). An octahedron-shaped colorless crystal with dimensions 0.08 × 0.08 × 0.06 mm^3 was sealed in a 0.5 mm OD glass number 50 (borosilicate glass) capillary tube with MiTeGen MicroTools before mounted onto a goniometer head. The data were collected under ambient temperature.

A cubic unit cell with dimensions $a = b = c = 24.8328(3)$ Å, $\alpha = \beta = \gamma = 90$ °, was derived from the least-square refinement of 9016 reflections in the range of $3.083 < \theta < 68.080$. Centrosymmetric space group *Fm-3* was initially assigned using XPREP[1] based on intensity statistics and the systematic absences.

The data were collected to 0.81 Å, and truncated to 0.83 Å for integration by Bruker program SAINT, empirical absorption correction was applied using program SADABS. The structure was solved with direct method using SHELXS and refined by full-matrix least-squares on F^2 using SHELXL[2] in Olex2[3]. All the Dy, O atoms and some C atoms were located easily, the rest of the C atoms were generated via subsequent difference Fourier syntheses.

All the non-H atoms were refined anisotropically. SIMU and DELU were applied to the C atoms. ISOR was applied to O1 and C3 atoms. DFIX was applied to some carbon-carbon bonds. After initial refinements, ADDSYM operation in PLATON[4] was used to convert the structure to a higher symmetry (*Fm-3m*), and transformation matrix [0 1 0 1 0 0 0 0 -1] was applied. The structure was finally refined and converged in the new space group.

Responses to checkCIF alerts:

RFACR01_ALERT_3_A The value of the weighted R factor is > 0.45

Weighted R factor given 0.545

PLAT084_ALERT_3_A High wR2 Value (i.e., > 0.25) .... 0.55 Report

Response: wR2 is large because the quality of the diffraction data is sub-optimal. However, the refinements converge well and yield a completely reasonable structure, comparable with previously reported similar structure involving Zr(IV)[5].

PLAT601_ALERT_2_A Structure Contains Solvent Accessible VOIDS of 9635 Ang^3

Response: The sample is a porous metal-organic framework material and the volume of the void is reasonable. There are severely disordered solvent molecules that cannot be crystallographically located residing in the void(s).

Table S1 Crystal data and structure refinement for **Dy^{3+}-NDC**

Identification code	lc70521rt_0m	
CCDC deposition number	1840493	
Empirical formula	C144 Dy12 O64	
Formula weight	4703.44	
Temperature	280(2) K	
Wavelength	1.54178 Å	
Crystal system	Cubic	
Space group	*Fm-3m*	
Unit cell dimensions	*a* = 24.8328(3) Å	*α* = 90°
	b = 24.8328(3) Å	*β* = 90°
	c = 24.8328(3) Å	*γ* = 90°
Volume	15313.6(3) Å^3	
Z	2	
Density (calculated)	1.020 mg/m^3	
Absorption coefficient	15.735 mm^{-1}	
F(000)	4335	
Crystal size	0.08 × 0.08 × 0.06 mm^3	
Theta range for data collection	3.08 to 68.31°.	
Index ranges	-27<=h<=29, -29<=k<=26, -29<=l<=29	
Reflections collected	23178	
Independent reflections	758 [R(int) = 0.0671]	
Completeness to theta = 68.31°	99.1 %	
Absorption correction	Semi-empirical from equivalents	
Max. and min. transmission	0.4520 and 0.3658	
Refinement method	Full-matrix least-squares on F^2	
Data / restraints / parameters	758 / 58 / 45	
Goodness-of-fit on F^2	2.986	
Final R indices [I>2sigma(I)]	R1 = 0.1562, wR2 = 0.5328	
R indices (all data)	R1 = 0.1623, wR2 = 0.5450	
Largest diff. peak and hole	2.276 and -6.265 e.Å^{-3}	

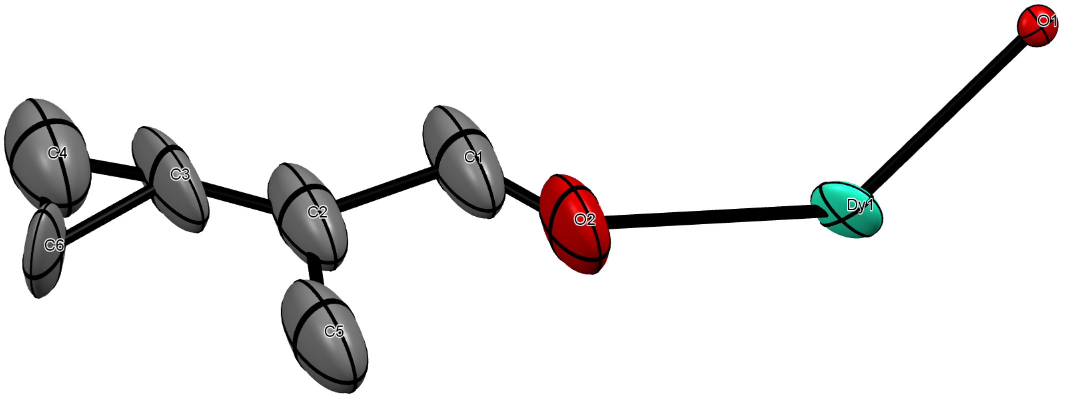

Fig. S2 ORTEP diagram of the asymmetric unit of **Dy^{3+}-NDC** (50% probability factor for the thermal ellipsoids), generated via Mercury 3.6[6].

2.5 SC-XRD of Dy^{3+}-BPDC MOF

X-ray diffraction data of **Dy^{3+}-BPDC** were collected on a Bruker X8 Prospector Ultra equipped with an Apex II CCD detector and an IμS micro-focus CuK\α source (λ = 1.54178 Å). An octahedron-shaped colorless crystal with dimensions 0.10 × 0.06 × 0.06 mm^3 was mounted on a goniometer head using MiTeGen MicroMesh. The data were collected under N_2 stream at 240K.

A cubic unit cell with dimensions $a = b = c = 27.5659$ (2) Å, $\alpha = \beta = \gamma = 90$ °, was derived from the least-square refinement of 9965 reflections in the range of $2.777 < \theta < 66.544$. Centrosymmetric space group *Fm-3m* was determined based on intensity statistics and the systematic absences.

The data were collected and integrated to 0.84 Å by Bruker program SAINT, empirical absorption correction was applied using program SADABS. The structure was solved with direct method using SHELXT[7] and refined by full-matrix least-squares on F^2 using SHELXL[2] in Olex2[3]. All the Dy, O atoms and some C atoms were located easily, the rest of the C atoms were generated via subsequent difference Fourier syntheses. Idealized atom positions were calculated for H atoms (d-(C-H) = 0.950 Å).

All the non-H atoms were refined anisotropically. All the H atoms were refined isotropically.

Response to checkCIF alert:

PLAT601_ALERT_2_A Structure Contains Solvent Accessible VOIDS of 13424 Ang^3

Response: The sample is a porous metal-organic framework material and the volume of the void is reasonable. There are severely disordered solvent molecules that cannot be crystallographically located residing in the void(s).

Table S2 Crystal data and structure refinement for **Dy^{3+}-BPDC**

Identification code	Ic61245_0m	
CCDC deposition number	1840494	
Empirical formula	C42 H24 Dy3 O20	
Formula weight	1336.11	
Temperature	240(2) K	
Wavelength	1.54178 Å	
Crystal system	Cubic	
Space group	*Fm-3m*	
Unit cell dimensions	a = 27.5659(2) Å	α = 90°
	b = 27.5659(2) Å	β = 90°
	c = 27.5659(2) Å	γ = 90°
Volume	20946.7(3) Å^3	
Z	8	
Density (calculated)	0.847 mg/m^3	
Absorption coefficient	11.571 mm^{-1}	
F(000)	5072	
Crystal size	0.10 × 0.06 × 0.06 mm^3	
Theta range for data collection	2.78 to 66.54°.	
Index ranges	-23<=h<=32, -31<=k<=31, -32<=l<=32	
Reflections collected	21680	
Independent reflections	990 [R(int) = 0.0785]	
Completeness to theta = 66.54°	99.9 %	
Absorption correction	Semi-empirical from equivalents	
Max. and min. transmission	0.5436 and 0.3908	
Refinement method	Full-matrix least-squares on F^2	
Data / restraints / parameters	990 / 0 / 40	
Goodness-of-fit on F^2	1.357	
Final R indices [I>2sigma(I)]	R1 = 0.0562, wR2 = 0.1854	
R indices (all data)	R1 = 0.0633, wR2 = 0.1926	
Largest diff. peak and hole	1.922 and -0.668 e.Å^{-3}	

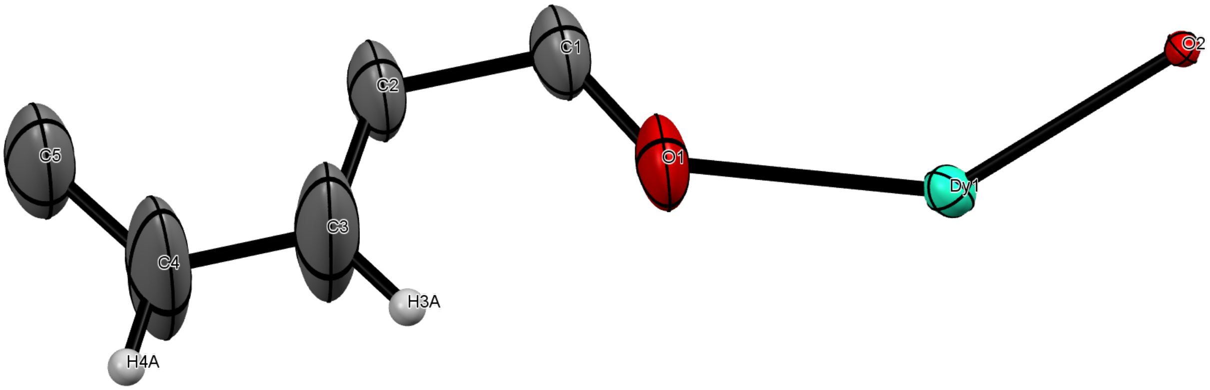

Fig. S3 ORTEP diagram of the asymmetric unit of **Dy^{3+}-BPDC** (50% probability factor for the thermal ellipsoids), generated via Mercury 3.6[6].

2.6 SC-XRD of Dy^{3+}-ABDC MOF

X-ray diffraction data of **Dy^{3+}-ABDC** were collected on a Bruker X8 Prospector Ultra equipped with an Apex II CCD detector and an IμS micro-focus CuK\α source (λ = 1.54178 Å). An octahedron-shaped orange-colored crystal with dimensions 0.12 × 0.12 × 0.08 mm^3 was mounted on a goniometer head using MiTeGen MicroMesh. The data were collected under N_2 stream at 240K.

A cubic unit cell with dimensions $a = b = c = 29.9107(6)$ Å, $\alpha = \beta = \gamma = 90$ °, was derived from the least-square refinement of 9865 reflections in the range of $4.174 < \theta < 68.296$. Centrosymmetric space group Fm-3m was determined based on intensity statistics and the systematic absences.

The data were collected to 0.81 Å and truncated to 0.83 Å for integration by Bruker program SAINT, empirical absorption correction was applied using program SADABS. The structure was solved with direct method using SHELXT[7] and refined by full-matrix least-squares on F^2 using SHELXL[2] in Olex2[3]. All the Dy, O atoms and some C atoms were located easily, the rest of the non-H atoms were generated via subsequent difference Fourier syntheses. Idealized atom positions were calculated for H atoms (d-(C-H) = 0.950 Å).

All the non-H atoms were refined anisotropically. All the H atoms were refined isotropically. ADP and rigid bond restraints were applied to the C and N atoms using SIMU and DELU commands. DFIX was also used to restrain some of the bond lengths.

Responses to checkCIF alerts:

PLAT430_ALERT_2_A Short Inter D...A Contact O1 .. O1 .. 2.49 Ang.

Response: The $Dy_6(OH)_8$ is a reasonable SBU structure which is also present in many other MOF structures reported in this dissertation as well as published literature, and the 2.49 Å inter-atomic distance is consistent with those values.

PLAT602_ALERT_2_A VERY LARGE Solvent Accessible VOID(S) in Structure

Response: The sample is a porous metal-organic framework material and the very large void is reasonable. There are severely disordered solvent molecules that cannot be crystallographically located residing in the void(s).

Table S3 Crystal data and structure refinement for **Dy^{3+}-ABDC**

Identification code	lc70513_0m	
CCDC deposition number	1840495	
Empirical formula	C42 H24 Dy3 N6 O16	
Formula weight	1356.17	
Temperature	240(2) K	
Wavelength	1.54178 Å	
Crystal system	Cubic	
Space group	*Fm-3m*	
Unit cell dimensions	a = 29.9107(6) Å	*α* = 90°
	b = 29.9107(6) Å	*β* = 90°
	c = 29.9107(6) Å	*γ* = 90°
Volume	26759.6(9) Å^3	
Z	8	
Density (calculated)	0.673 mg/m^3	
Absorption coefficient	9.052 mm^{-1}	
F(000)	5152	
Crystal size	0.12 × 0.12 × 0.08 mm^3	
Theta range for data collection	2.56 to 68.54°.	
Index ranges	-36<=h<=35, -36<=k<=31, -23<=l<=36	
Reflections collected	43329	
Independent reflections	1293 [R(int) = 0.1647]	
Completeness to theta = 68.54°	99.9 %	
Absorption correction	Semi-empirical from equivalents	
Max. and min. transmission	0.5312 and 0.4097	

Refinement method	Full-matrix least-squares on F^2
Data / restraints / parameters	1293 / 48 / 41
Goodness-of-fit on F^2	1.203
Final R indices [I>2sigma(I)]	R1 = 0.0529, wR2 = 0.1535
R indices (all data)	R1 = 0.0581, wR2 = 0.1606
Largest diff. peak and hole	1.117 and -1.219 e.Å^{-3}

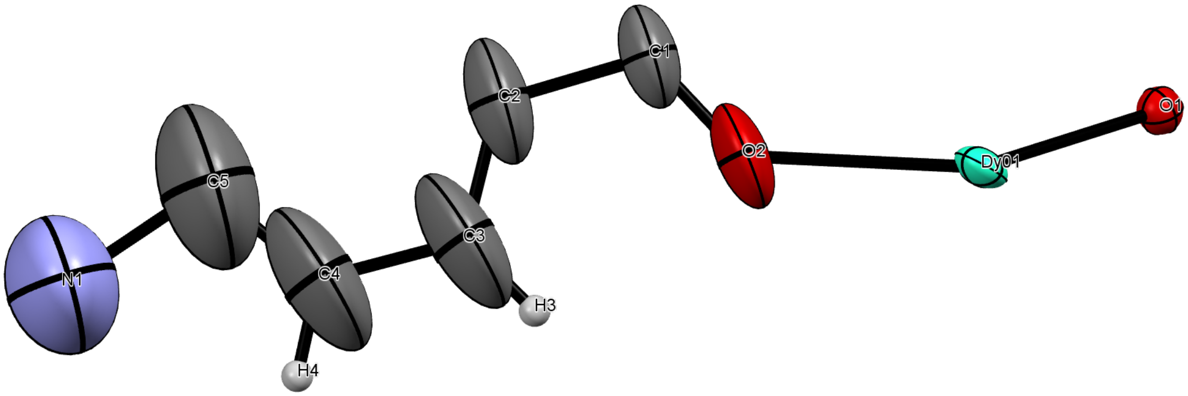

Fig. S4 ORTEP diagram of the asymmetric unit of **Dy^{3+}-ABDC** (50% probability factor for the thermal ellipsoids), generated via Mercury 3.6[6].

2.7 PXRD of fcu Dy^{3+}-MOFs

For PXRD, the as-synthesized MOFs were washed with dry DMF (3X), soaked at 75 °C for 10 min, washed with dry DMF (3X), soaked at 75 °C for another 10 min, washed and stored under dry DMF. PXRD experiments were run on crystals which were placed on glass slides with excess DMF removed.

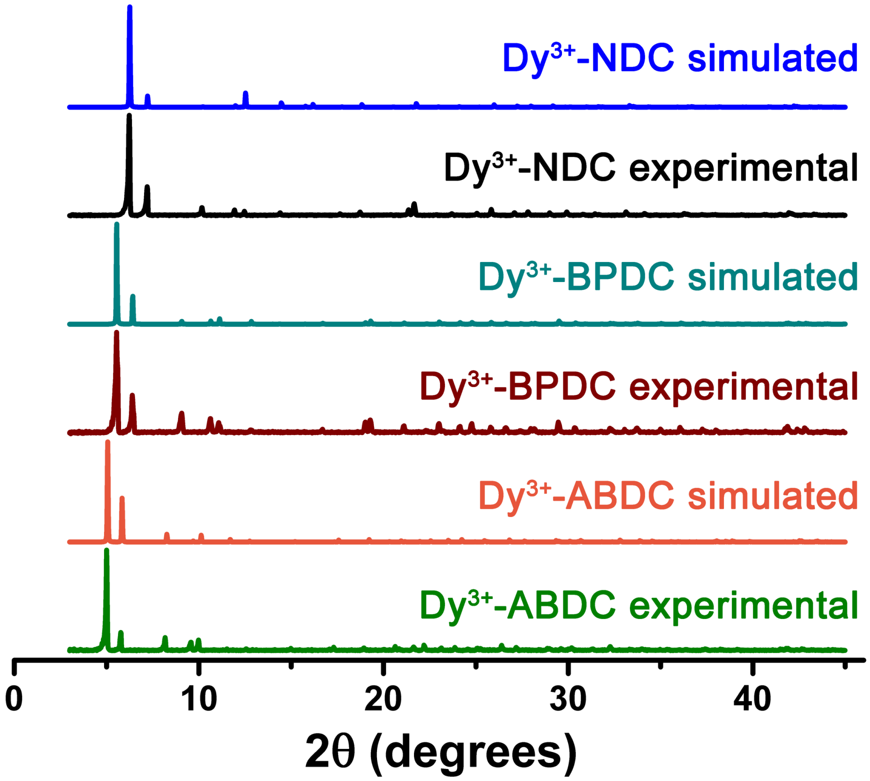

Fig. S5 Comparison of simulated and experimental PXRD patterns of three **fcu** Dy^{3+}-MOFs.

2.8 CHN elemental analysis and TGA of fcu Dy^{3+}-MOFs

For EA, MOF crystals were washed with dry DMF as previously described in 2.7, and dried with Ar flow until they became free-flowing solids. For TGA, the as-synthesized MOF crystals were washed with dry DMF, as previously described in 2.7, dried with Ar flow until they became free-flowing solids, and then loaded into a tared Pt pan for analysis.

Dy^{3+}-NDC, EA calculated % for $Dy_6(OH)_8(C_{12}H_6O_4)_6(C_2H_8N)_2 \cdot (DMF)_{10}(H_2O)_6$: C, 38.26; H, 4.3; N, 5.05. Found (%): C, 37.68; H, 3.8; N, 5.79.

Dy^{3+}-BPDC, EA calculated % for $Dy_6(OH)_8(C_{14}H_8O_4)_6(C_2H_8N)_2 \cdot (DMF)_{18}(H_2O)_1$: C, 42.83; H, 5.06; N, 7.03. Found (%): C, 43.05; H, 4.64; N, 6.36.

Dy^{3+}-ABDC, EA calculated % for $Dy_6(OH)_8(C_{14}H_8N_2O_4)_6(C_2H_8N)_2 \cdot (DMF)_{18}(H_2O)_{10}$: C, 39.59; H, 5.1; N, 10.4. Found (%): C, 38.48; H, 5.00; N, 11.2.[*]

---

[*] The formula for **Dy^{3+}-ABDC** given here considers an ideal crystal structure where there is no missing linker defect. After correlating EA and TGA results, it was suggested that there might be a significant percentage of the ABDC linkers missing from the ideal structure. A corrected formula and relevant discussion are in the footnote on page S17.

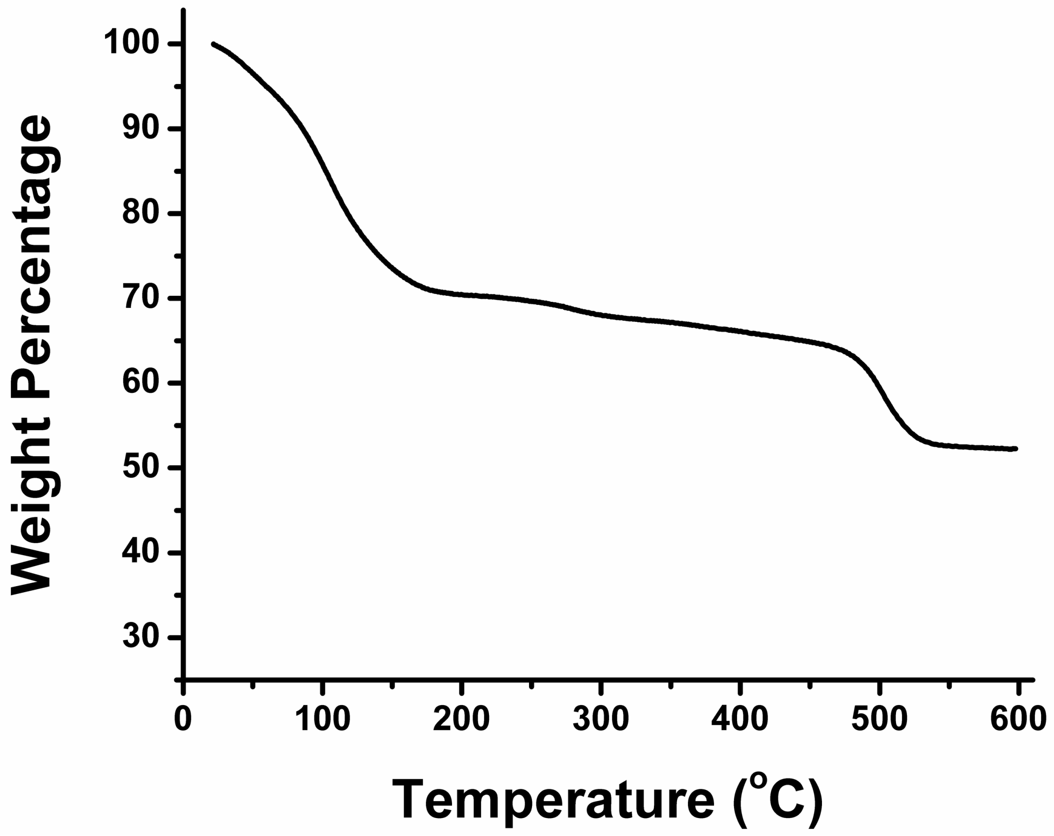

Fig. S6 TGA profile of **Dy^{3+}-NDC**. The major weight loss of 28.9% between r.t. and 175 °C corresponds to the loss of 10DMF and 6H_2O (calculated. 25.2%).[†]

[†] The discrepancy can be explained by the decomposition and removal of dimethylammonium counterions and dehydration of the $Dy_6(OH)_8$ clusters.

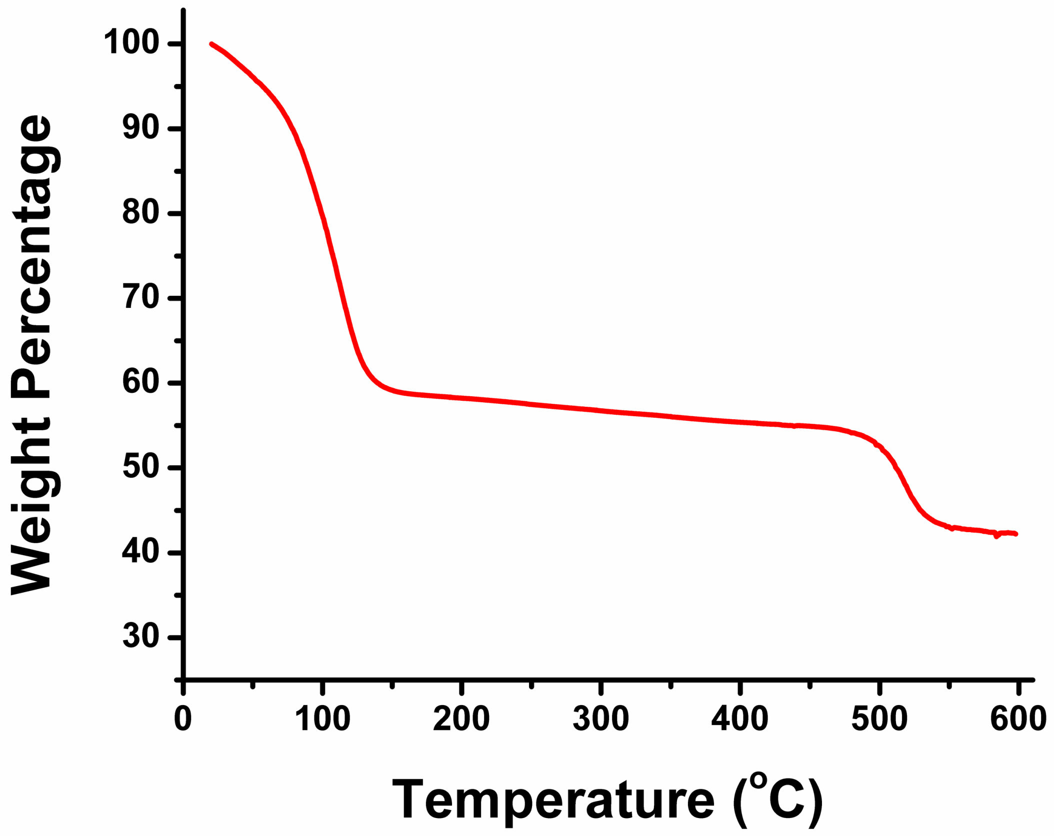

Fig. S7 TGA profile of **Dy^{3+}-BPDC**. The major weight loss of 40.9% between r.t. and 150 ºC corresponds to the loss of 18DMF and 1H_2O (calculated 33.5%).[‡]

[‡] The discrepancy can be explained by the decomposition and removal of dimethylammonium counterions and dehydration of the $Dy_6(OH)_8$ clusters.

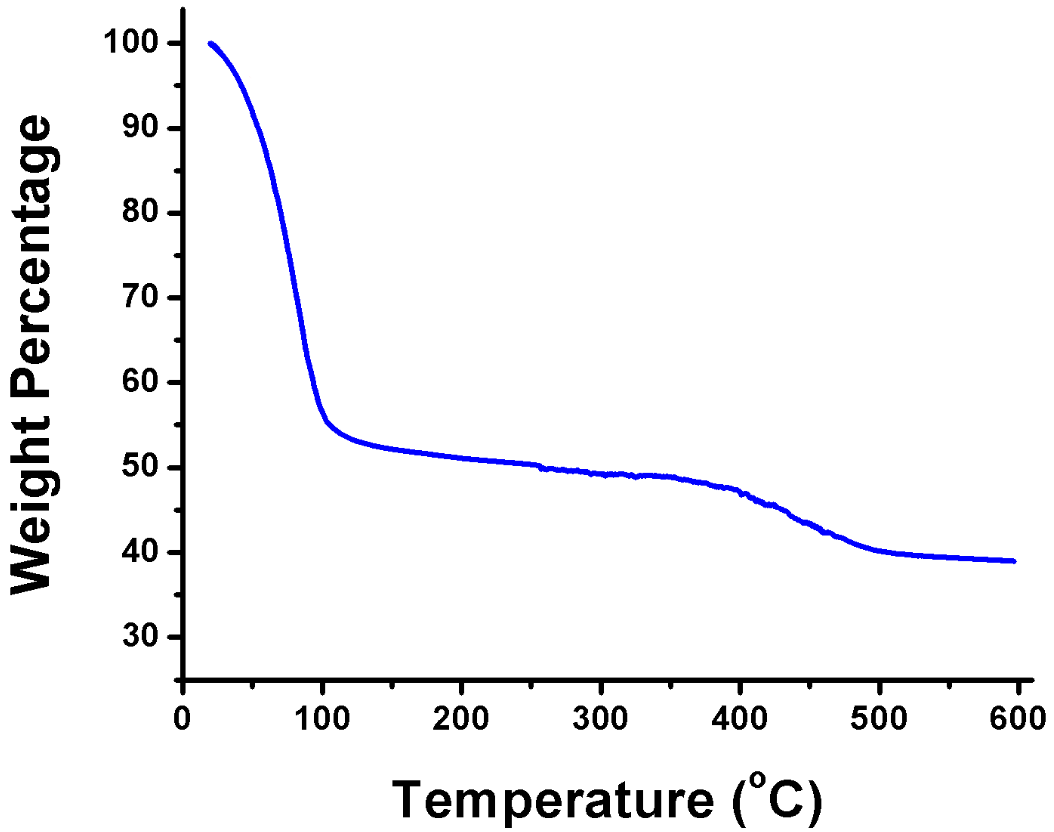

Fig. S8 TGA profile of **Dy^{3+}-ABDC**. The major weight loss of 47.8% between r.t. and 150 °C corresponds to the loss of 18DMF and 10H_2O (calculated 34.7%).[§]

[§] The discrepancy cannot be adequately explained by the decomposition and removal of dimethylammonium counterions and dehydration of the $Dy_6(OH)_8$ clusters. Therefore, it is possible that coordinative defects (missing ABDC linkers) are present as those observed for the Zr^{4+}-based MOFs. After taking missing linker defects into consideration, the formula of this batch of **Dy^{3+}-ABDC** MOF was corrected to $Dy_6(OH)_8(C_{14}H_8N_2O_4)_{5.1}(C_2H_8N)_{0.2}\cdot(DMF)_{23}(H_2O)_{11}$, calculated (%): C, 38.72; H, 5.39; N, 10.7. Found (%): C, 38.48; H, 5.00; N, 11.2. The loss of 23DMF and 11H_2O before 150 °C accounts for 43.0% of weight loss, which is in a better agreement with the TGA profile.

2.9 ^{1}H NMR of digested fcu Dy^{3+}-MOFs

For ^{1}H NMR, MOF crystals were washed with dry DMF as previously described in 2.7, and washed with DCM (3X), soaked in DCM at room temperature for 1 hour, washed again with DCM (3X), and dried with Ar flow. Dried MOF samples were dissolved in DMSO-d_6 (0.7 mL) and DCl in D_2O (37%, 0.01 mL) for ^{1}H NMR. As shown in Fig. S6, the product MOFs are free of DFBA.

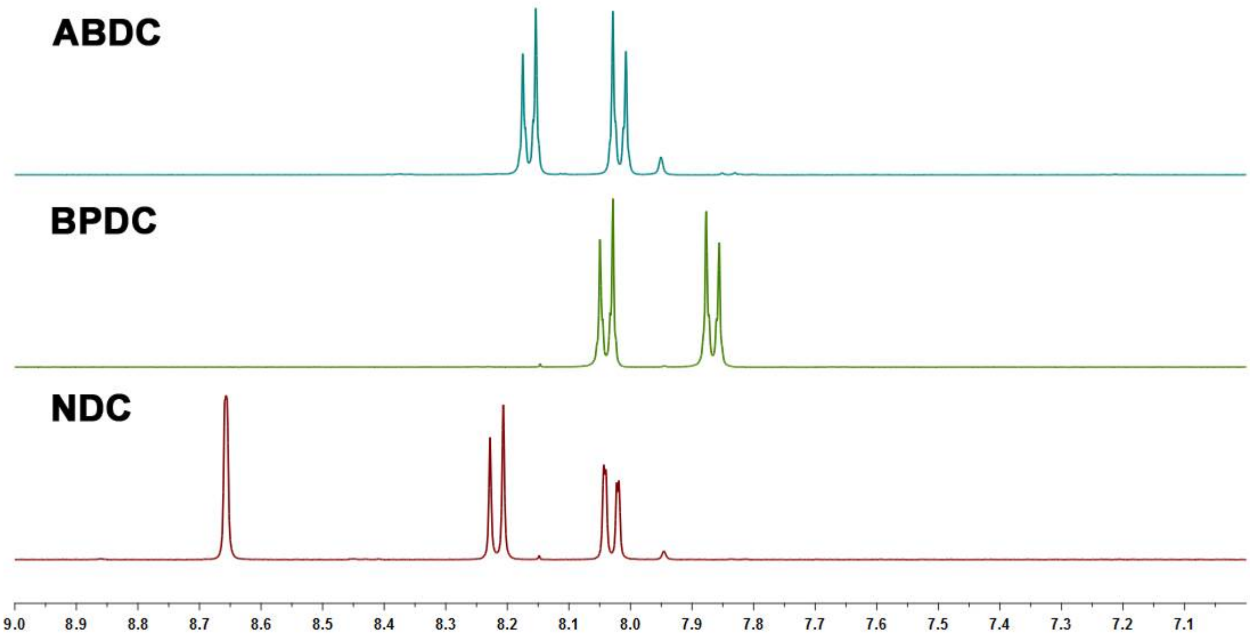

Fig. S9 ^{1}H NMR spectra of digested **Dy^{3+}-NDC** (bottom), **Dy^{3+}-BPDC** (middle), and **Dy^{3+}-ABDC** (top).

2.10 N_2 sorption of fcu Dy^{3+}-MOFs

The same activation procedure was performed on all three analogues, **Dy^{3+}-NDC**, **Dy^{3+}-BPDC**, and **Dy^{3+}-ABDC**: as-synthesized MOFs were washed with dry DMF, as described in 2.7, then solvent exchange with dry chloroform was performed, followed by dynamic vacuum pumping.

For **Dy^{3+}-ABDC**, a supercritical CO_2 activation protocol was also attempted (with no significant difference from the chloroform-exchanged sample): as-synthesized **Dy^{3+}-ABDC** crystals were washed with dry DMF, as described in 2.7, then exchanged with dry EtOH for 3 days in a 20 mL vial. EtOH was removed every 8 hours followed by replenishment with fresh EtOH. The crystals were then transferred to the activation chamber of a Tousimis SAMDRI-PVT-3B supercritical drier where supercritical CO_2 activation experiment was performed. During the entire transfer process, all the crystals were soaked under dry EtOH. After cooling to 0 °C, the chamber was filled with liquid CO_2. Every 30 min, the chamber was purged for 5 min, while the CO_2 filling rate was kept above the purge rate to ensure that the MOF sample remains soaked under liquid CO_2. The chamber temperature was kept between 0−10 °C. After 6 hours, the chamber filled with liquid CO_2 was heated to 40 °C to transform CO_2 from liquid state to supercritical state. The chamber was then vented slowly for the next 18 hours until the pressure dropped down to 1 atm. The MOF sample was then degassed at 50 °C under dynamic vacuum for 24 hours before the N_2 adsorption experiment was performed.

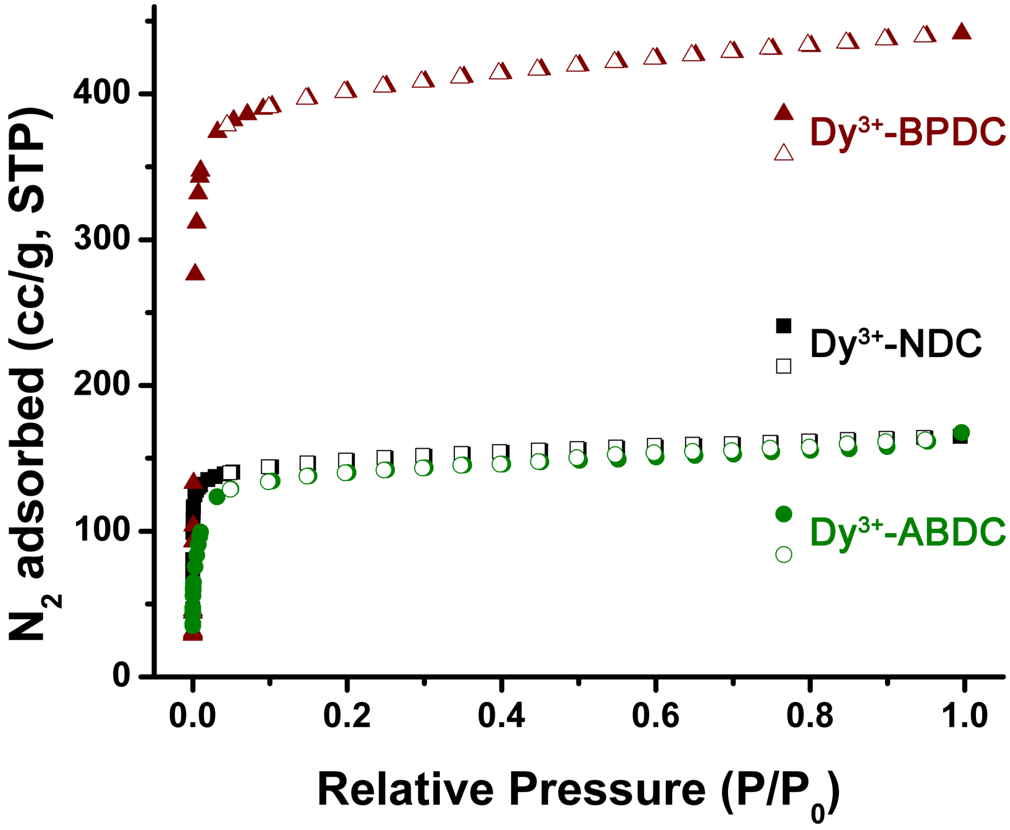

Fig. S10 N_2 isotherms at 77 K of **Dy^{3+}-NDC**, **Dy^{3+}-BPDC**, and **Dy^{3+}-ABDC**.

2.12 PXRD of fcu rare earth MOFs

For PXRD, the as-synthesized MOFs were washed with dry DMF as described in 2.7. PXRD experiments were run on wet crystals which were placed on glass slides with excess DMF removed.

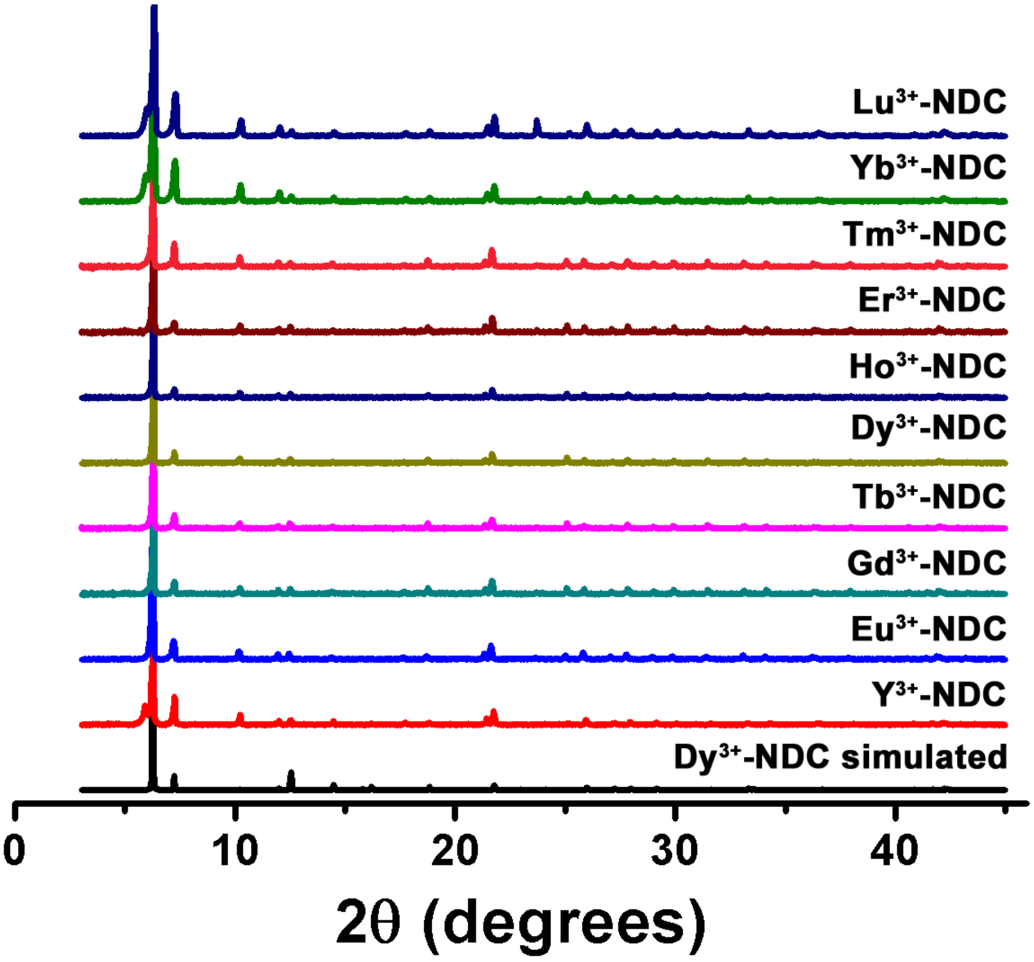

Fig. S11 Experimental PXRD patterns of 10 different **RE^{3+}-NDC** MOFs comparing to simulated **Dy^{3+}-NDC**.

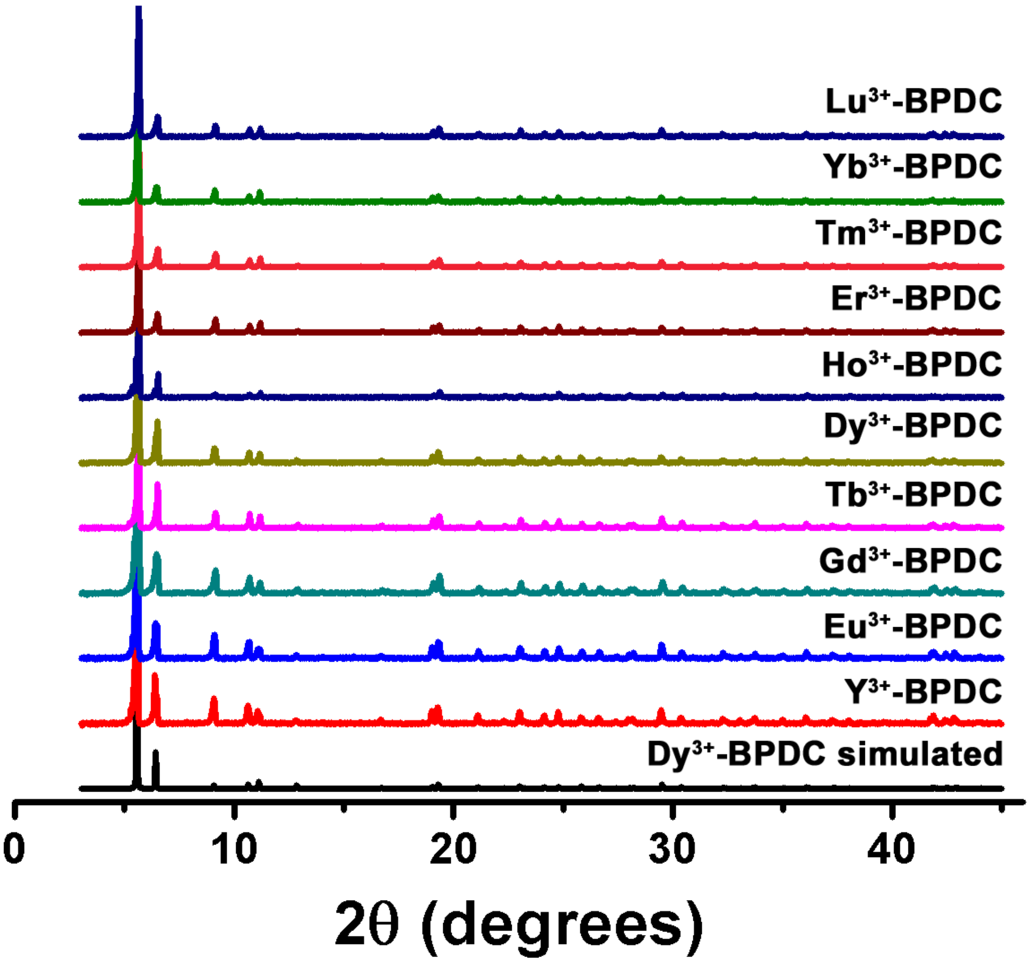

Fig. S12 Experimental PXRD patterns of 10 different **RE^{3+}-BPDC** MOFs comparing to simulated **Dy^{3+}-BPDC**.

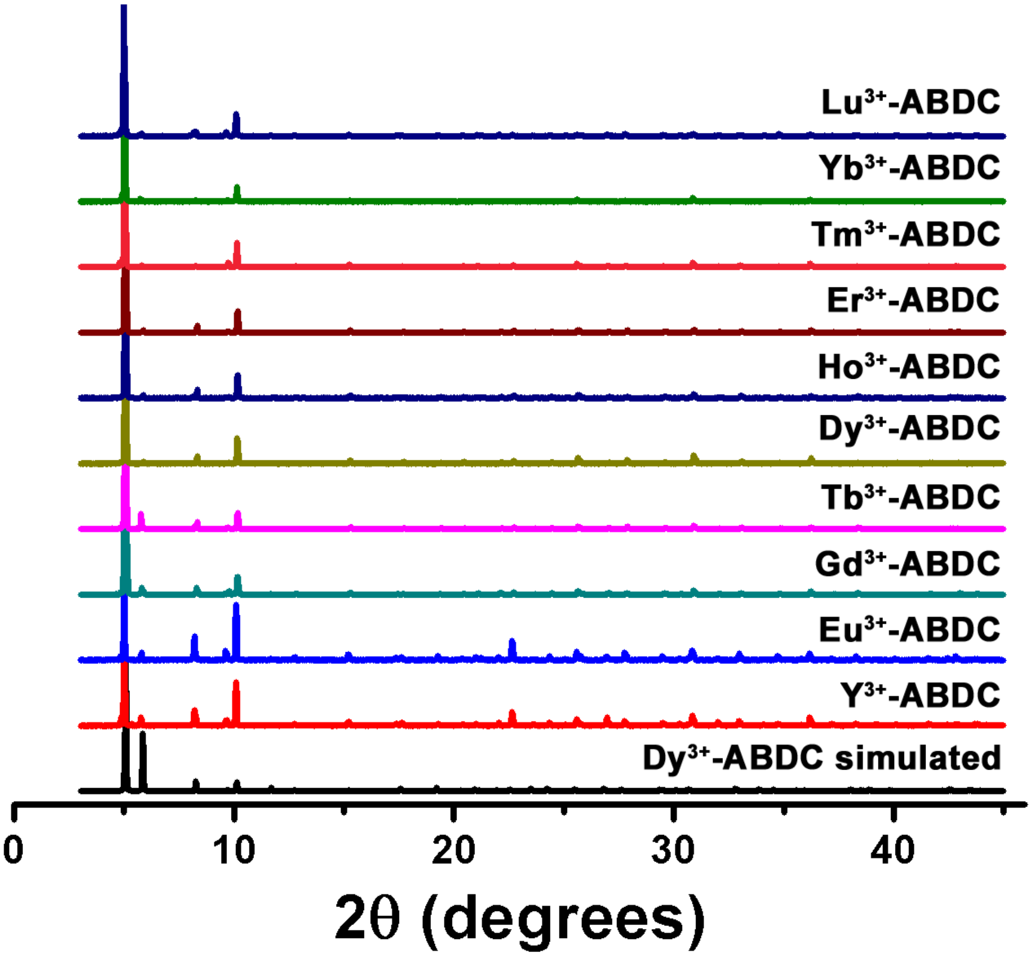

Fig. S13 Experimental PXRD patterns of 10 different **RE^{3+}-ABDC** MOFs comparing to simulated **Dy^{3+}-ABDC**.

3. Syntheses and characterization of dye-loaded MOFs

The as-synthesized MOF crystals were washed with dry DMF as previously described in 2.7, then washed with DMSO (3X, pre-dried over 4Å molecular sieves), soaked in DMSO for 1 hour, washed again with DMSO (3X) and kept under DMSO. Dye compounds were dissolved in DMSO with the aid of ultrasonication to achieve pre-determined concentrations. For Dy^{3+}-MOF incorporation, 5 mg of DMSO-exchanged MOF crystals were mixed with corresponding dye/DMSO solutions (0.5 mL, 10 mg/mL) and soaked at room temperature for 24 hours. The MOF crystals were then separated from the dye solutions via centrifugation and copiously washed with DMSO until the supernatant appeared colorless. PXRD were performed on the MOF crystals under DMSO (Fig. S13 to S15).

For ^1H NMR, the MOFs were then washed with DCM (5X), soaked in DCM for 1 hour, washed again with DCM (5X) and dried with Ar flow. The dried MOF samples were dissolved in DMSO-d_6 (0.7 mL) and DCl in D_2O (37%, 0.012 mL) for ^1H NMR. For comparison, pure dye compounds were also acidified and dissolved in DMSO-d_6 (0.7 mL) and DCl in D_2O (37%, 0.024 mL) for ^1H NMR. ^1H NMR spectra for **Dy^{3+}-NDC** treated with various dyes are shown in Fig. S18, to identify the additional peaks on the **LDS 698@Dy^{3+}-NDC** spectrum, comparison with pure LDS 698 is shown in Fig. S19. Similarly, ^1H NMR spectra for **Dy^{3+}-BPDC** after dye exchange reactions are shown in Fig. S20. A comparison of different **dye@Dy^{3+}-BPDC** samples with corresponding pure dye molecules is shown in Fig. S21 to S25. ^1H NMR spectra for various **dye@Dy^{3+}-ABDC** samples are shown in Fig. S26, and Fig. S27 to S31 can be used to help identify the presence and quantities of the dyes, by comparing with the spectra of the corresponding pure dye molecules.

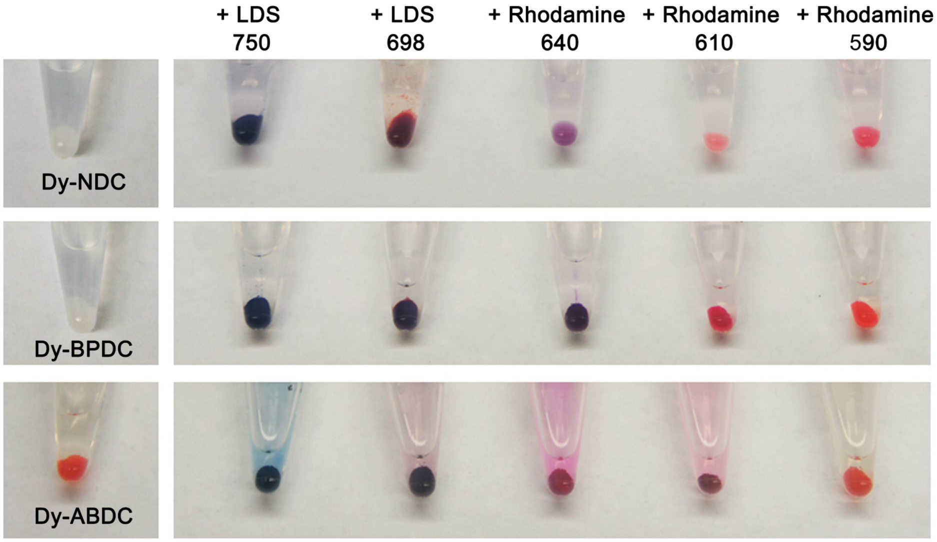

Fig. S14 Visible changes before and after loading various dyes into Dy^{3+}-MOFs via cation exchange

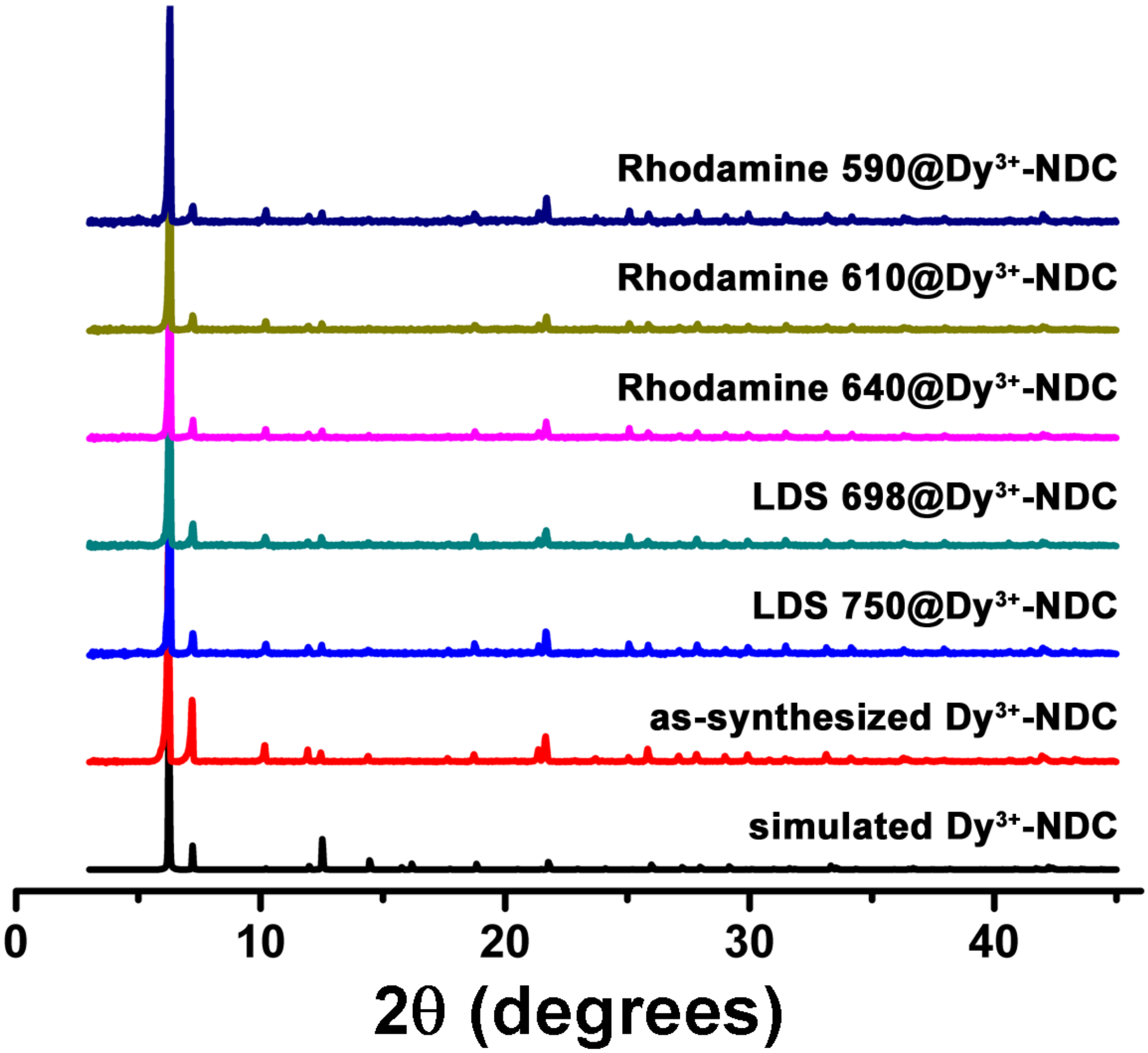

Fig. S15. Experimental PXRD patterns of 5 different dye-loaded **Dy^{3+}-NDC** MOFs comparing to as-synthesized and simulated **Dy^{3+}-NDC**.

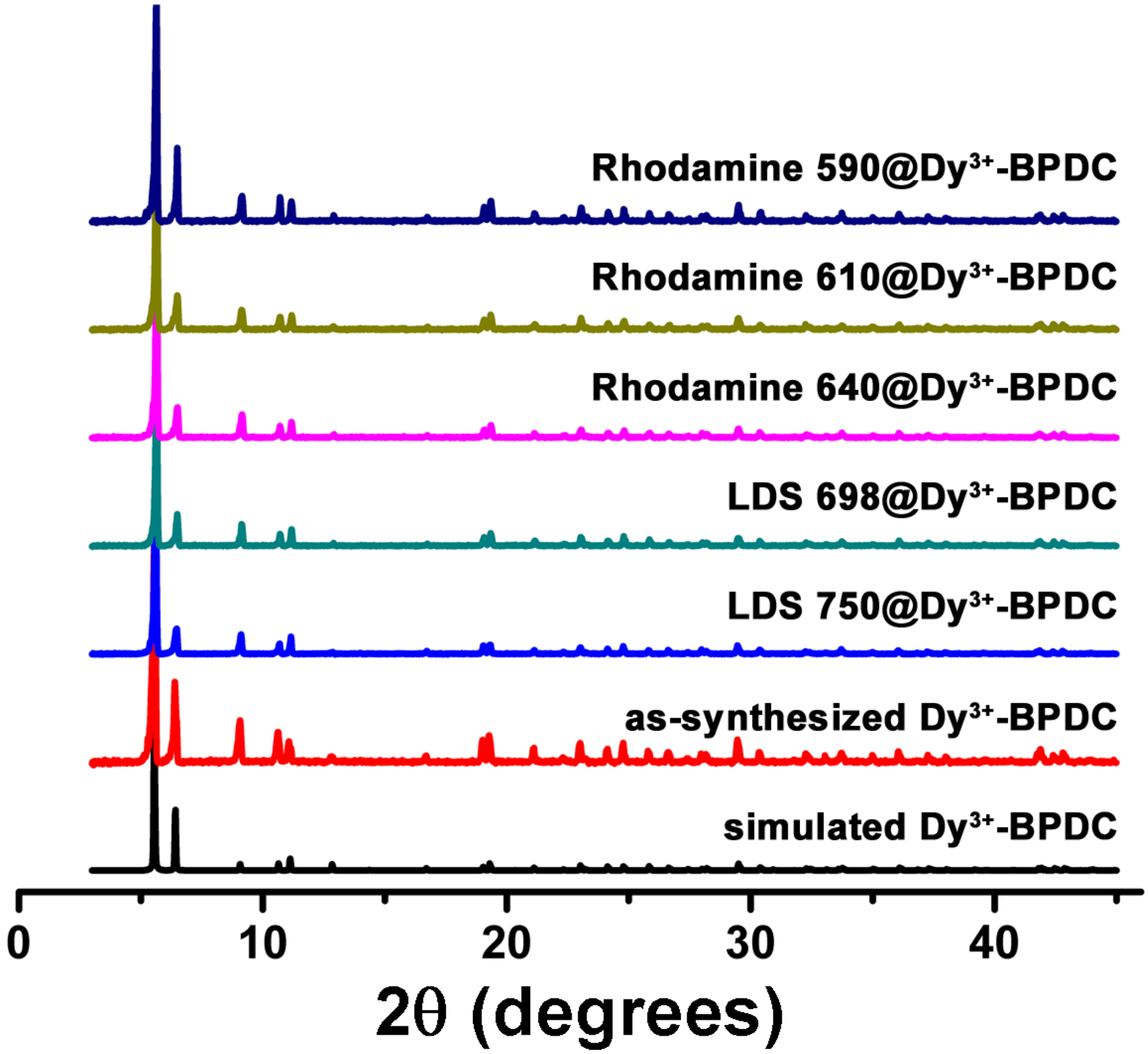

Fig. S16. Experimental PXRD patterns of 5 different dye-loaded **Dy^{3+}-BPDC** MOFs comparing to as-synthesized and simulated **Dy^{3+}-BPDC**.

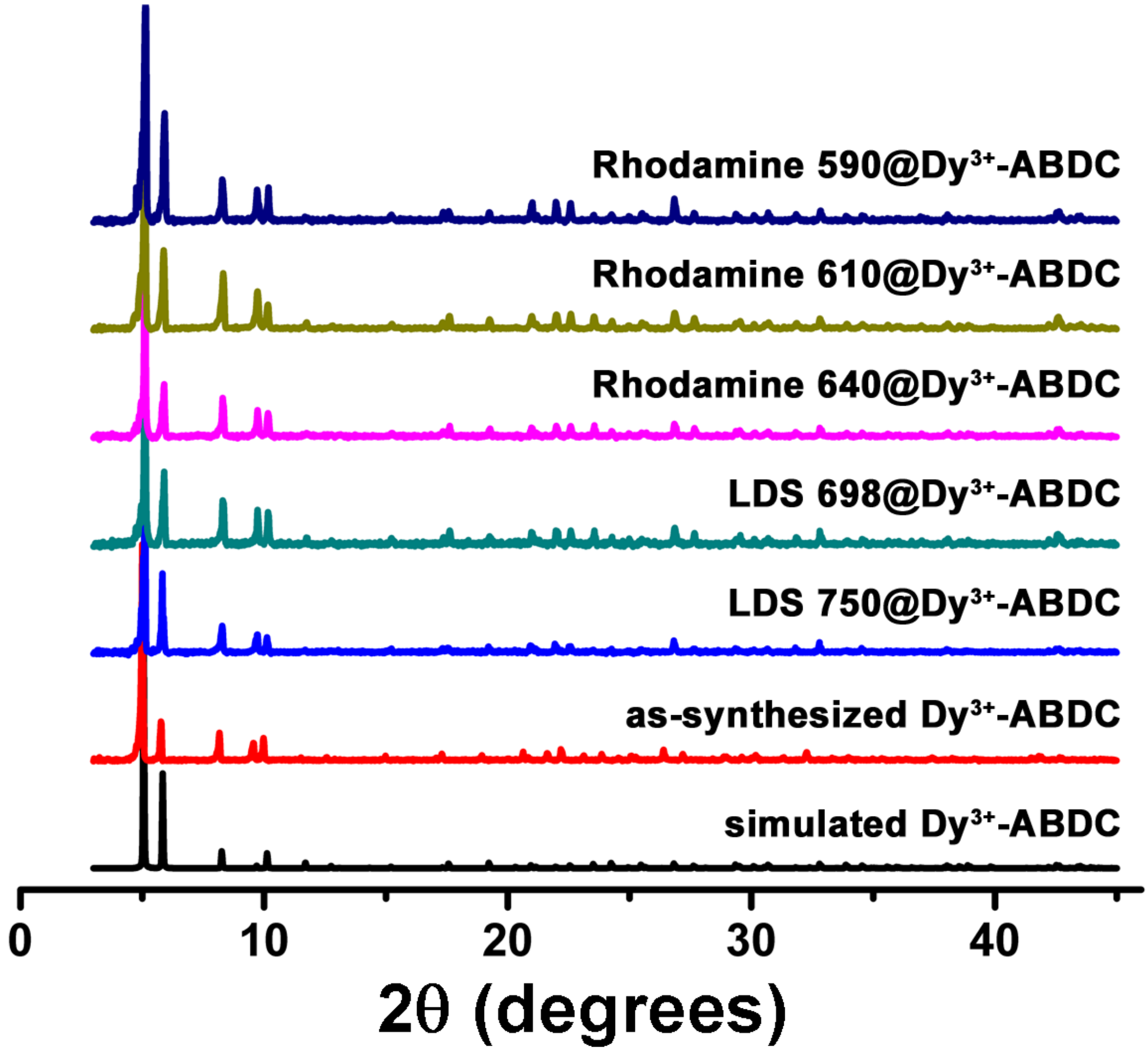

Fig. S17. Experimental PXRD patterns of 5 different dye-loaded **Dy^{3+}-ABDC** MOFs comparing to as-synthesized and simulated **Dy^{3+}-ABDC**.

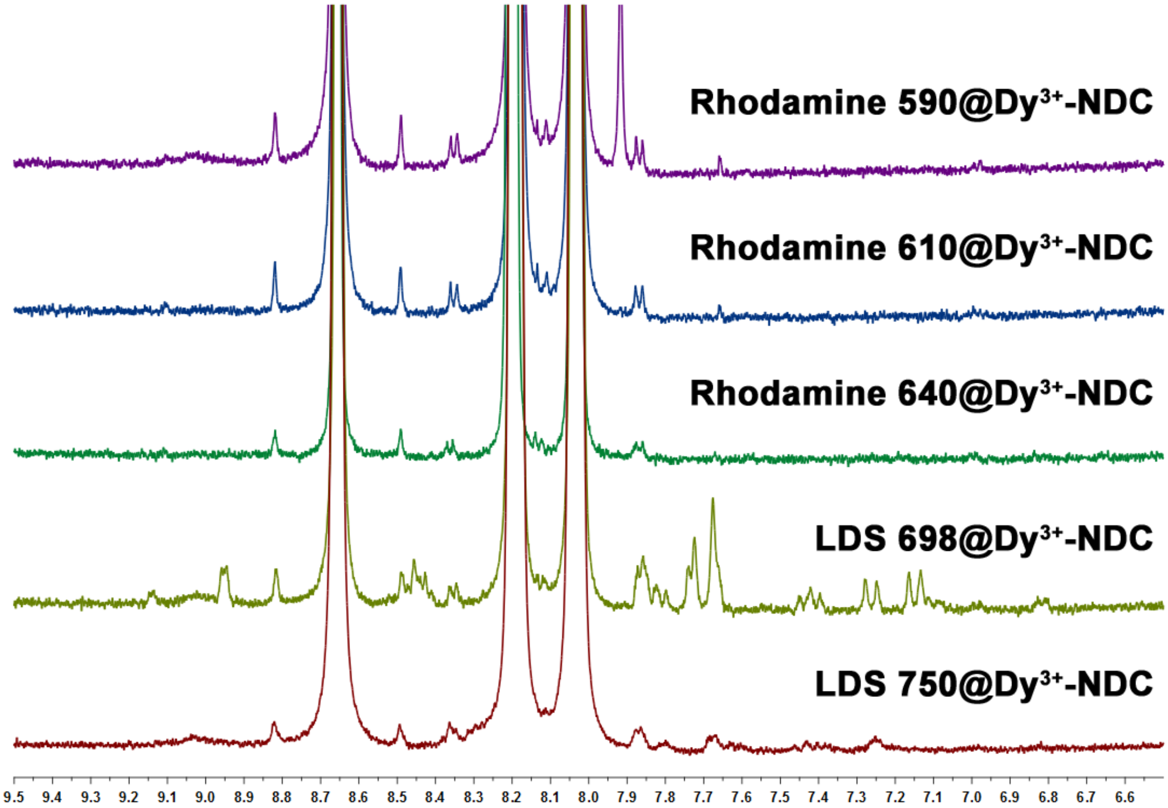

Fig. S18. ^{1}H NMR spectra of digested **Dy^{3+}-NDC** after treatments of various dyes.

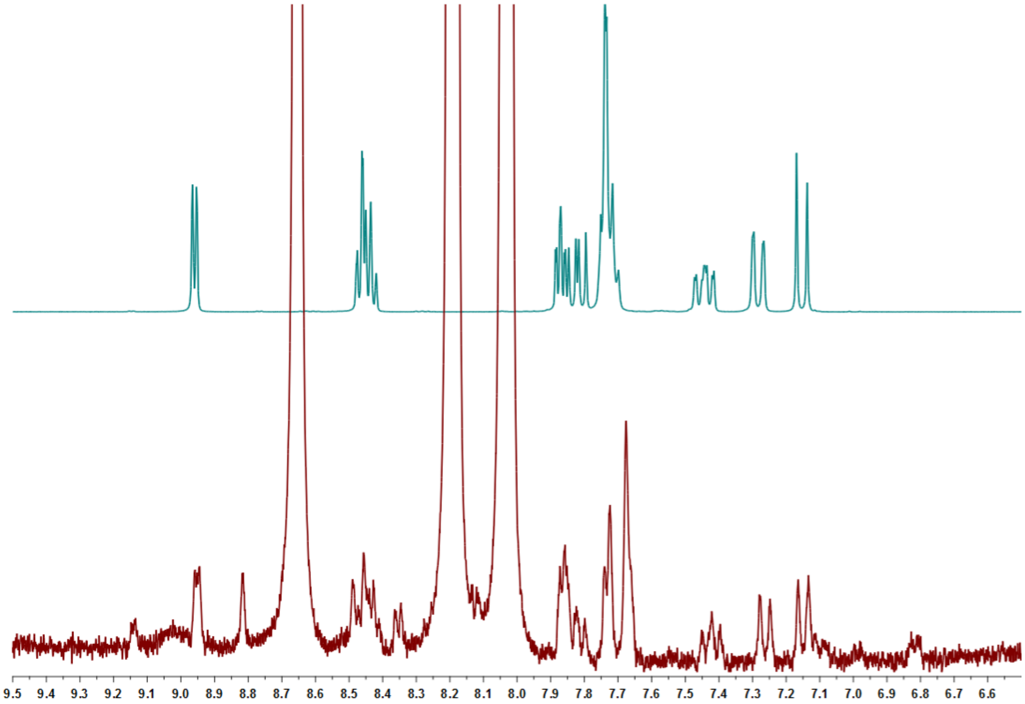

Fig. S19. ^{1}H NMR spectra of LDS 698 (top) and **LDS 698@Dy^{3+}-NDC** (bottom).

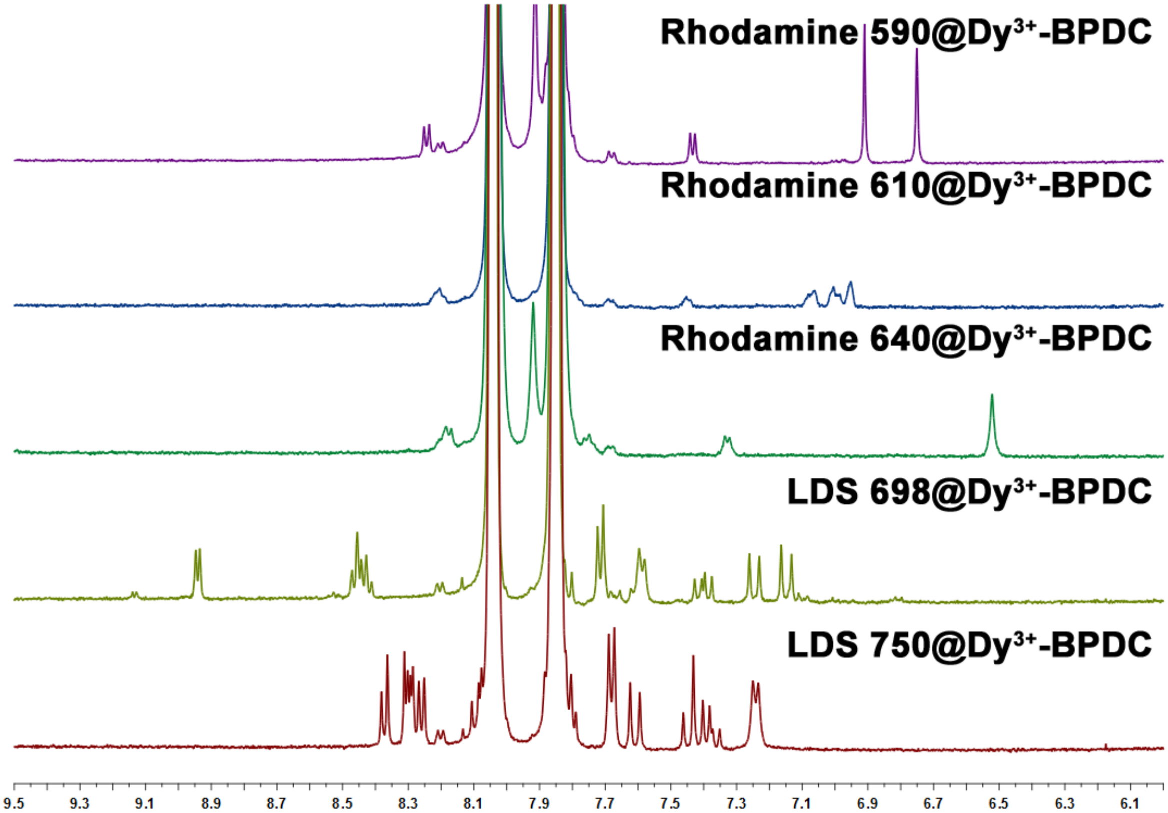

Fig. S20. ^{1}H NMR spectra of digested **Dy^{3+}-BPDC** after treatments of various dyes.

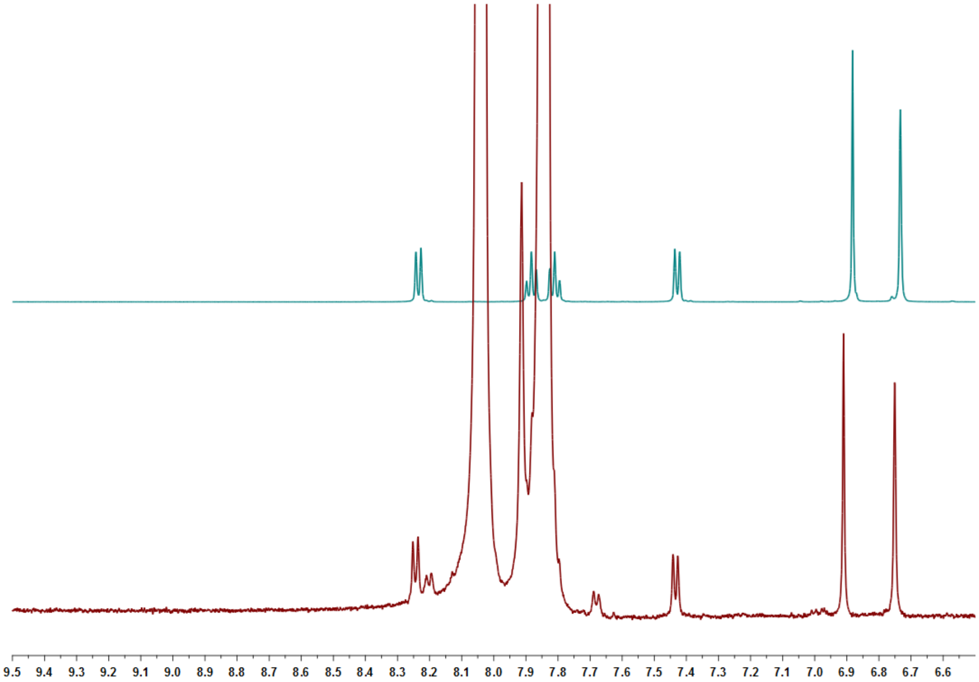

Fig. S21. ^{1}H NMR spectra of Rhodamine 590 (top) and **Rhodamine 590@Dy^{3+}-BPDC** (bottom).

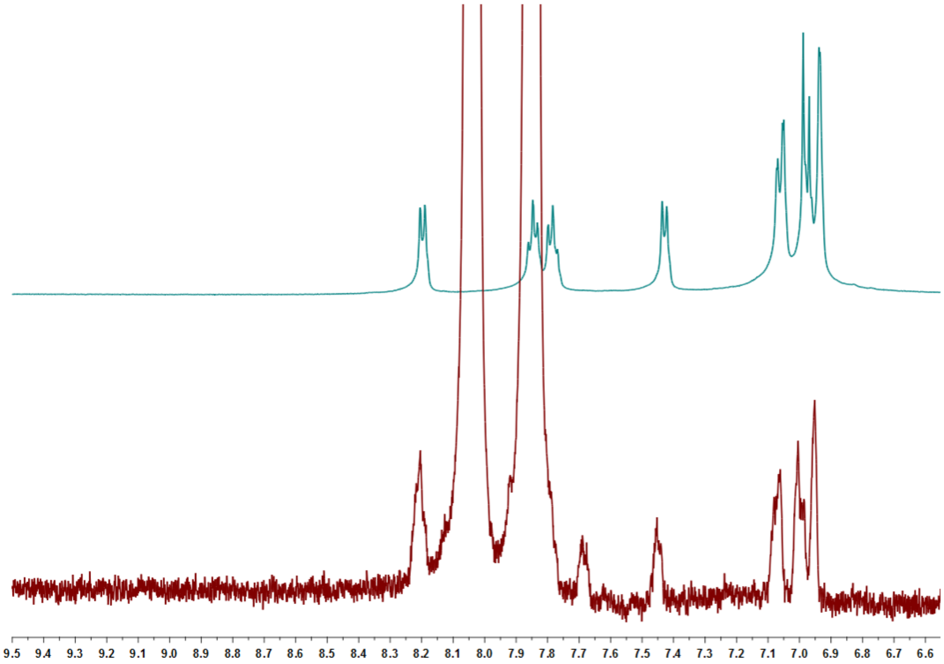

Fig. S22. ^{1}H NMR spectra of Rhodamine 610 (top) and **Rhodamine 610@Dy^{3+}-BPDC** (bottom).

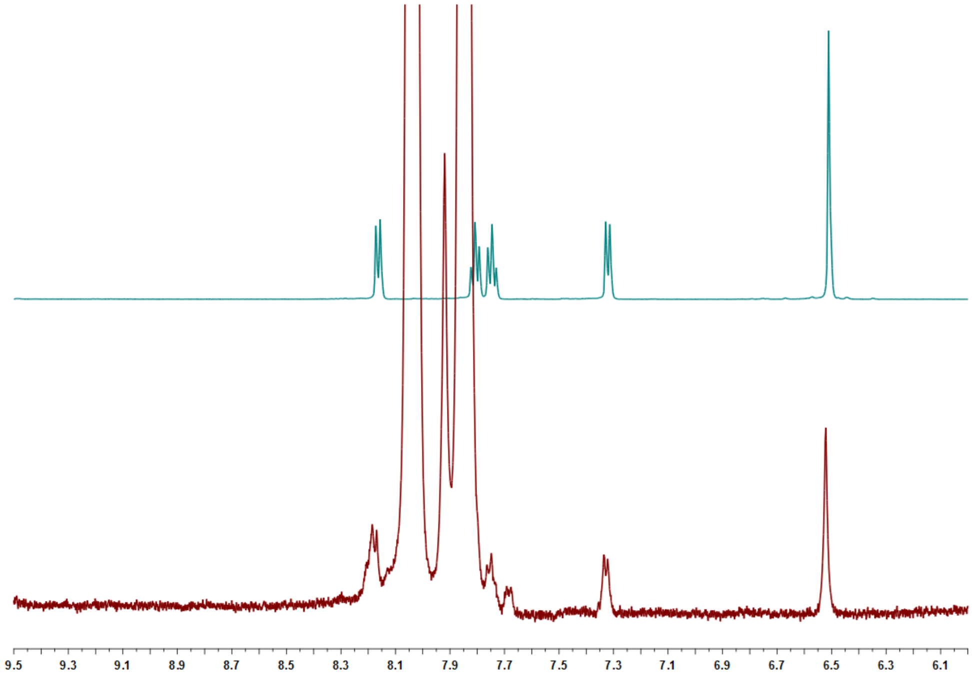

Fig. S23. ^{1}H NMR spectra of Rhodamine 640 (top) and **Rhodamine 640@Dy^{3+}-BPDC** (bottom).

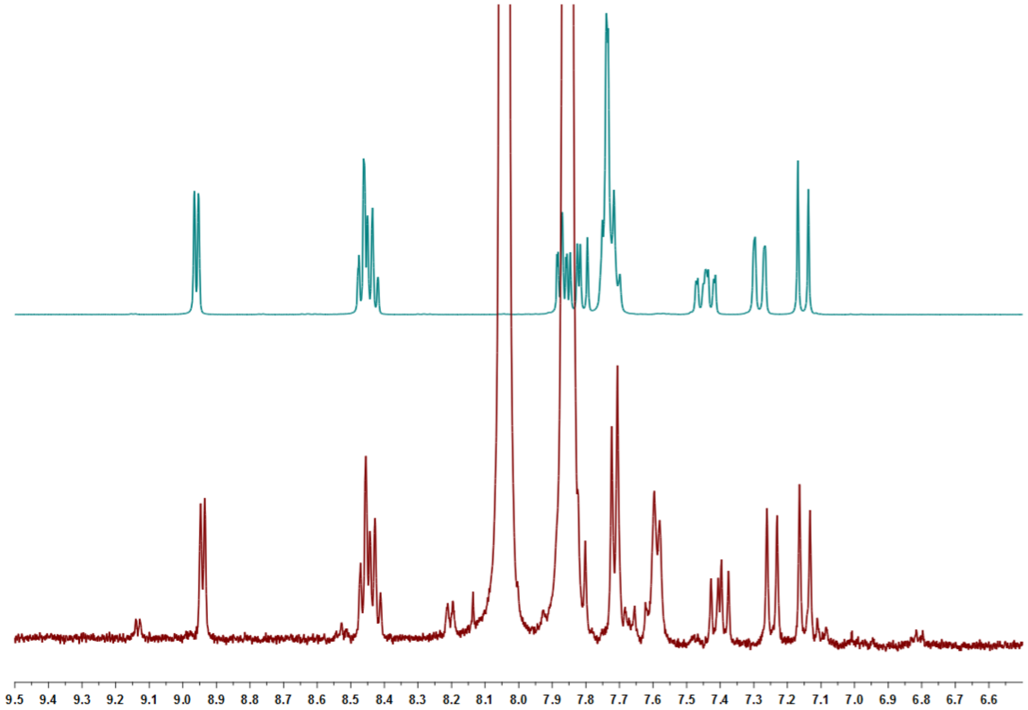

Fig. S24. ^{1}H NMR spectra of LDS 698 (top) and **LDS 698@Dy^{3+}-BPDC** (bottom).

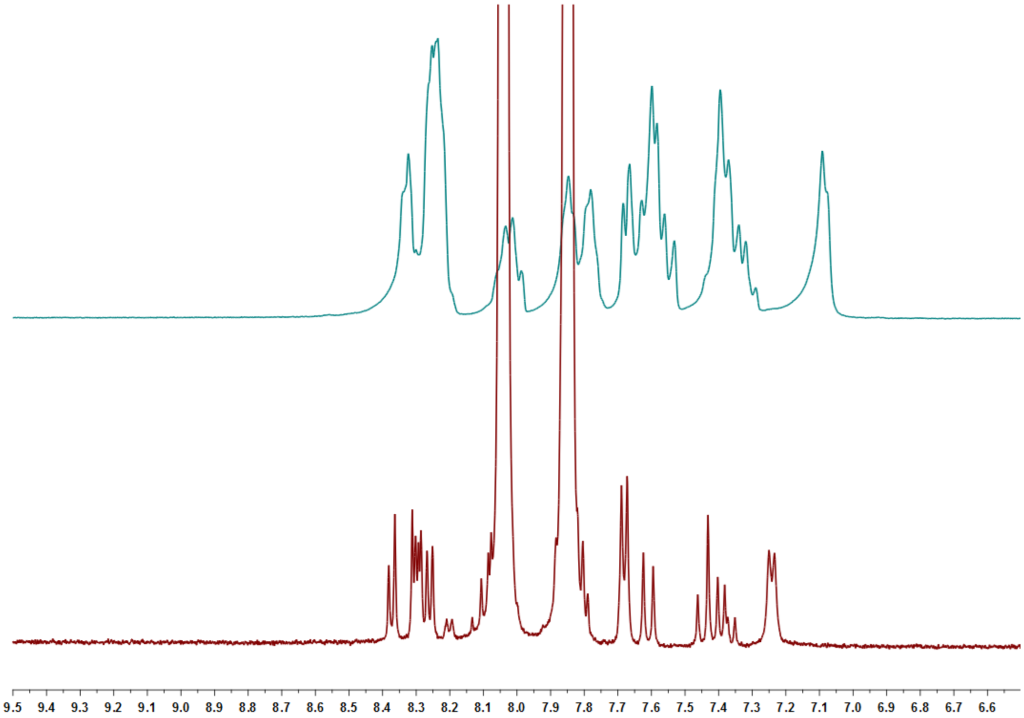

Fig. S25. ^{1}H NMR spectra of LDS 750 (top) and **LDS 750@Dy^{3+}-BPDC** (bottom).

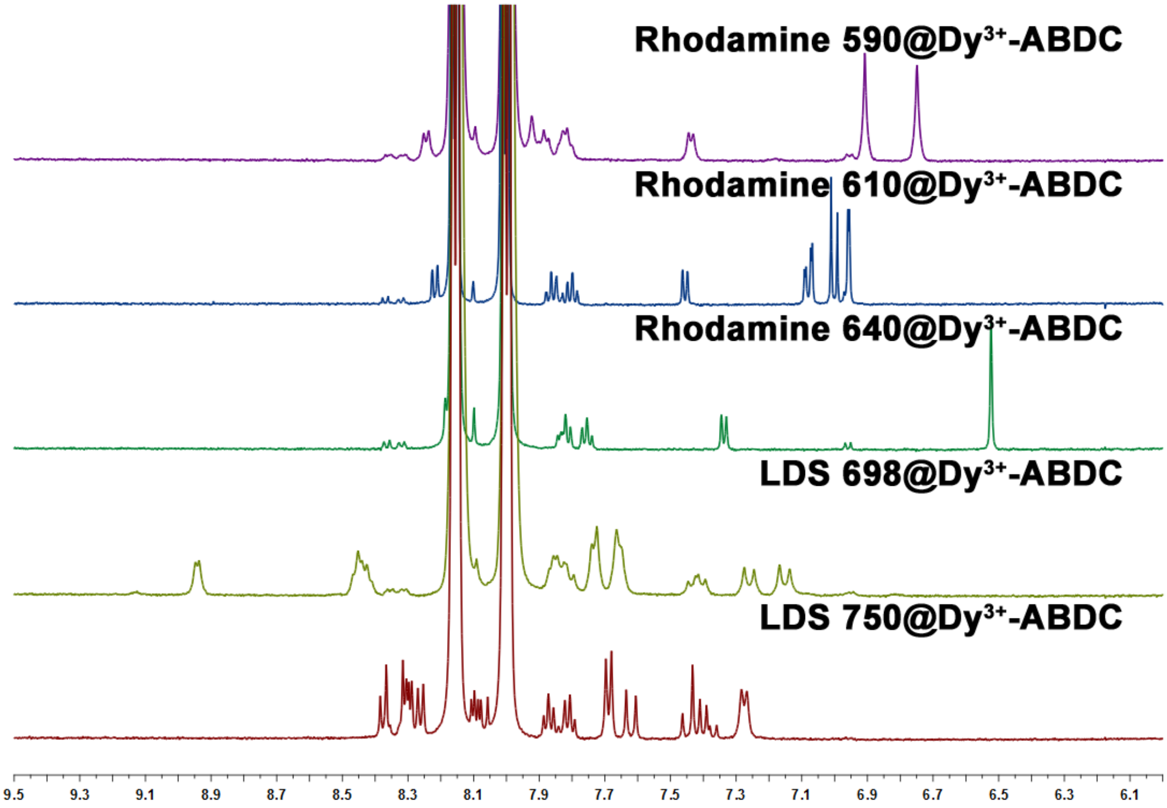

Fig. S26. ^{1}H NMR spectra of digested **Dy^{3+}-ABDC** after treatments of various dyes.

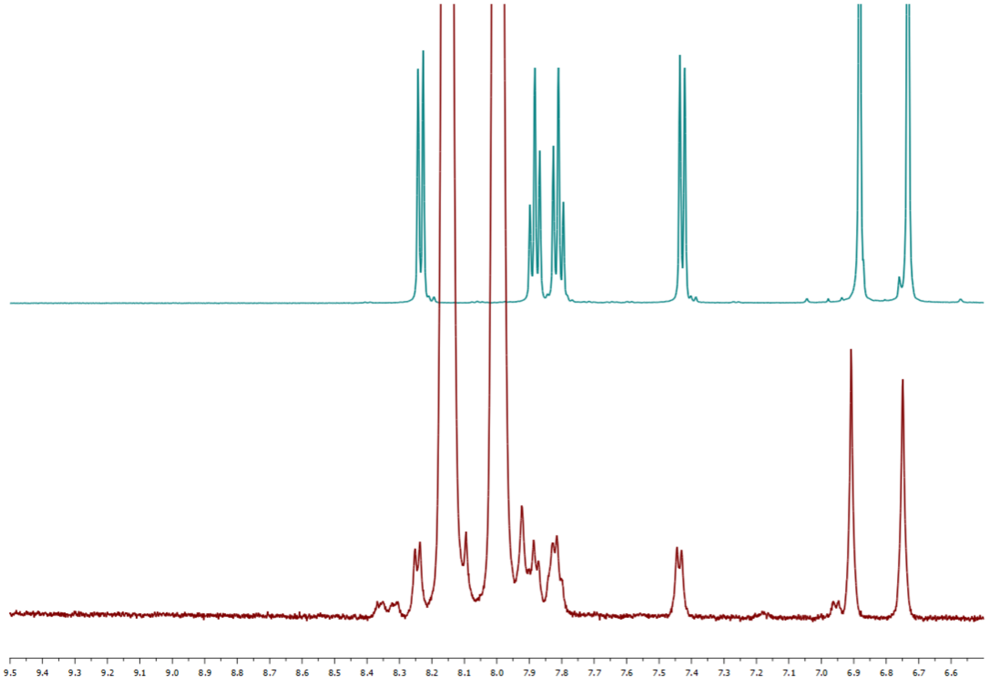

Fig. S27. ^{1}H NMR spectra of Rhodamine 590 (top) and **Rhodamine 590@Dy^{3+}-ABDC** (bottom).

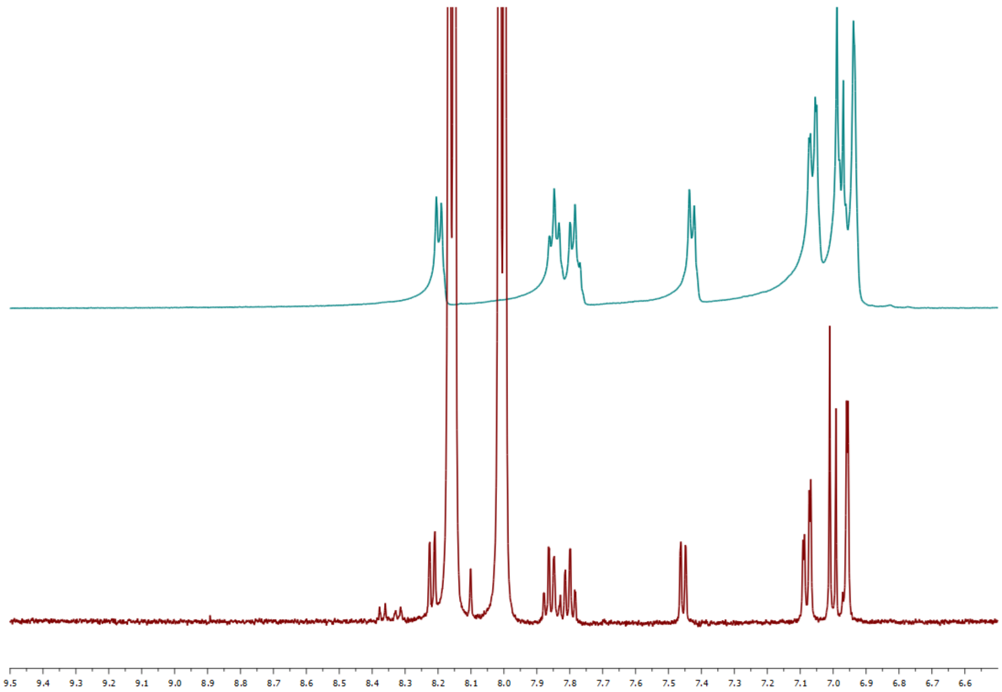

Fig. S28. ^{1}H NMR spectra of Rhodamine 610 (top) and **Rhodamine 610@Dy^{3+}-ABDC** (bottom).

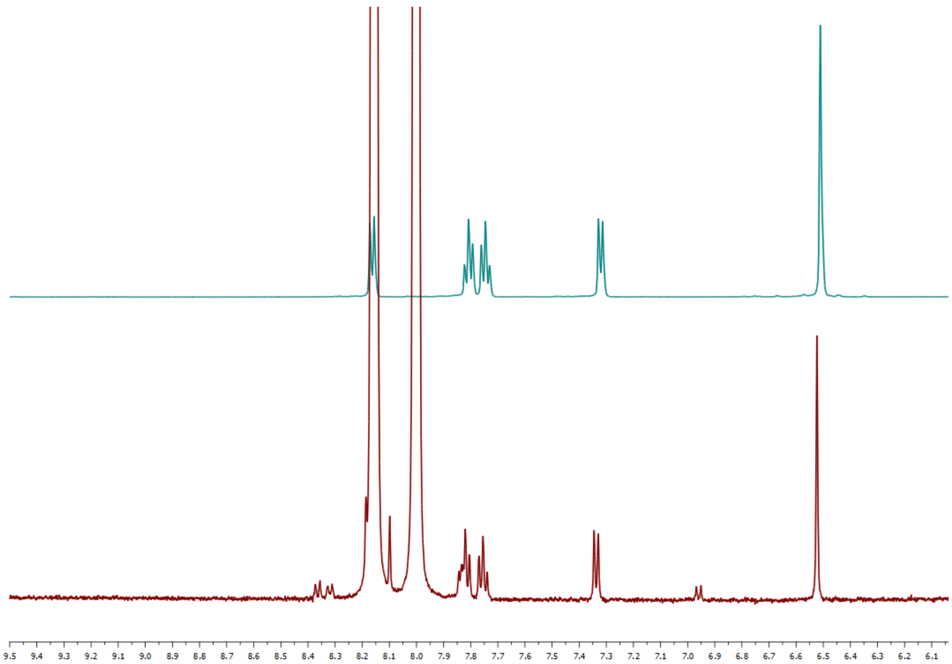

Fig. S29. ^{1}H NMR spectra of Rhodamine 640 (top) and **Rhodamine 640@Dy^{3+}-ABDC** (bottom).

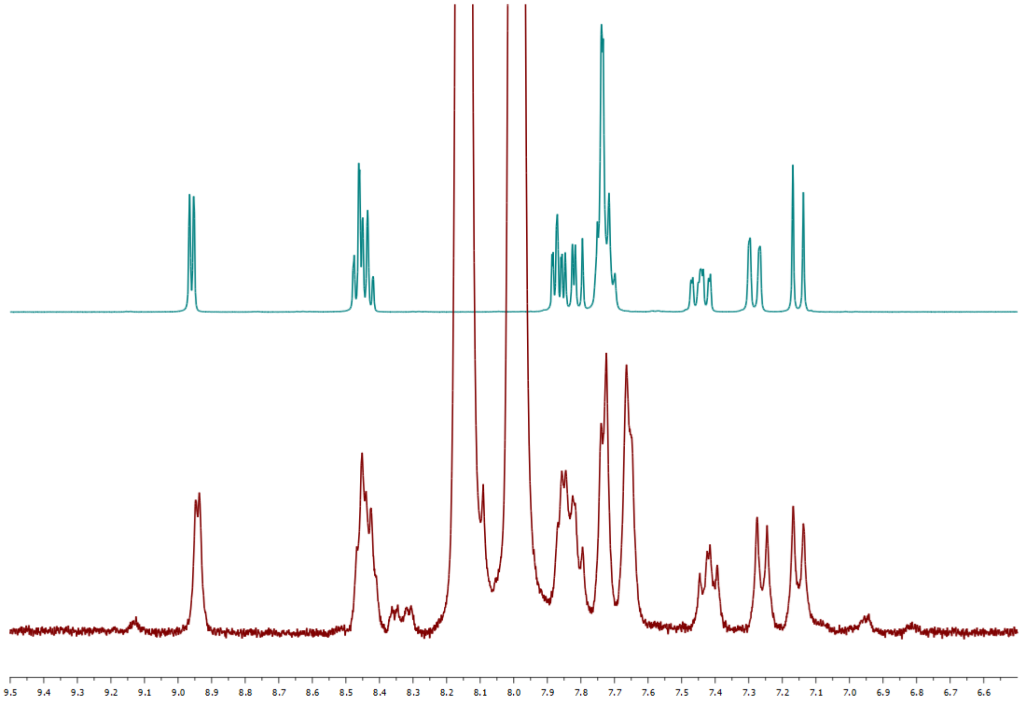

Fig. S30. ^{1}H NMR spectra of LDS 698 (top) and **LDS 698@Dy^{3+}-ABDC** (bottom).

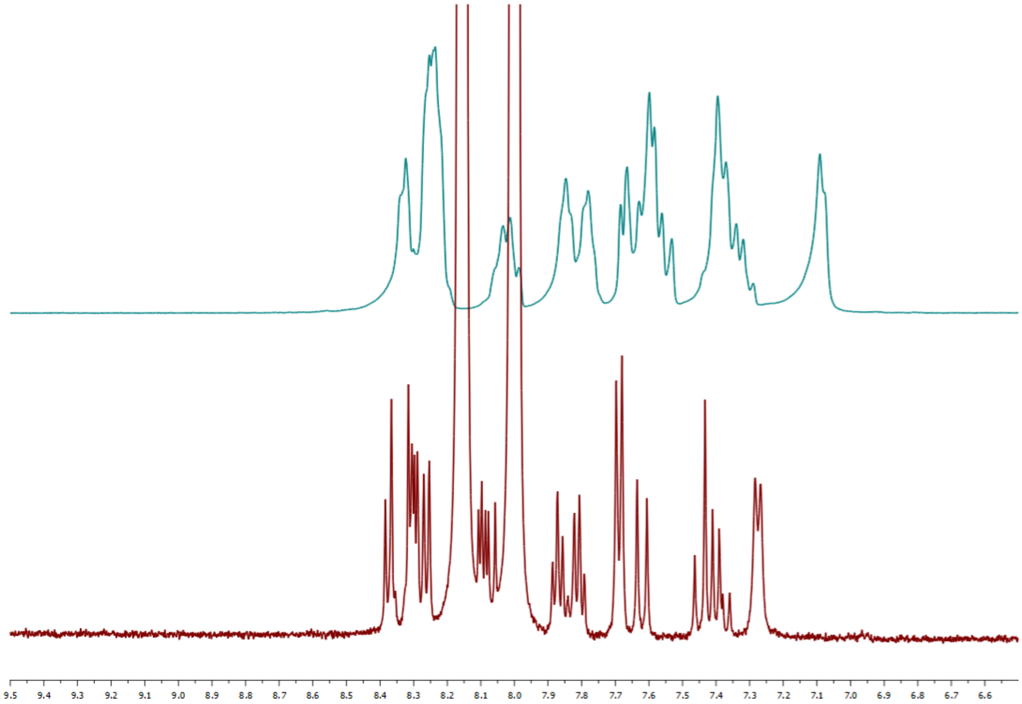

Fig. S31. ^{1}H NMR spectra of LDS 750 (top) and **LDS 750@Dy^{3+}-ABDC** (bottom).

4. Synthesis, characterization, and photoluminescence study of LDS 750@Yb^{3+}-BPDC MOF

Yb^{3+}-BPDC was prepared as described in 2.2, and washed with DMF and DCM, using the protocol for ^{1}H NMR sample preparation described in 2.9.

LDS 750@Yb^{3+}-BPDC was prepared using the protocol described in section 3, however with the concentration of the LDS 750 solution and soaking time varied (Fig. S32). It was then washed with DMSO and DCM, using the protocol for ^{1}H NMR sample preparation described in section 3.

The samples (**Yb^{3+}-BPDC** and **LDS 750@Yb^{3+}-BPDC**) were then dried in Ar flow before briefly ground with MgO powder (2-5 wt.% MOF) using mortar and pestle. PXRD was used to confirm the retention of crystallinity after grinding (Fig. S33).

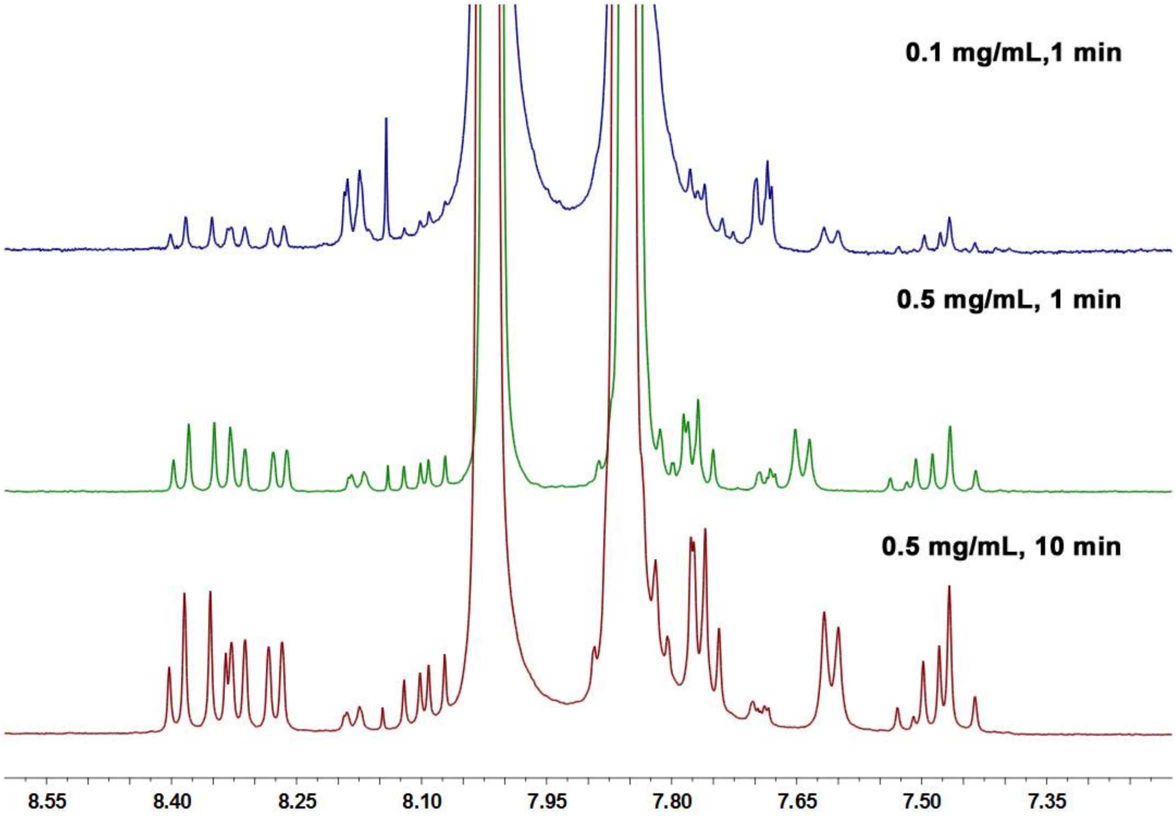

Fig. S32. ^{1}H NMR spectra of digested **Yb^{3+}-BPDC** loaded with different amounts of LDS 750[**]

[**] The peaks at the leftmost which correspond to one of the LDS 750 alkenyl groups were used to compare with the highest peak which is from BPDC.

Table S4 Different Yb^{3+} : LDS 750 ratios from different synthetic conditions based on ^{1}H NMR analysis of digested **LDS 750@Yb^{3+}-BPDC**

Condition	Yb^{3+} : LDS 750
0.1 mg/mL, 1 min	1 : 0.003
0.5 mg/mL, 1 min	1 : 0.03
0.5 mg/mL, 10 min	1 : 0.06

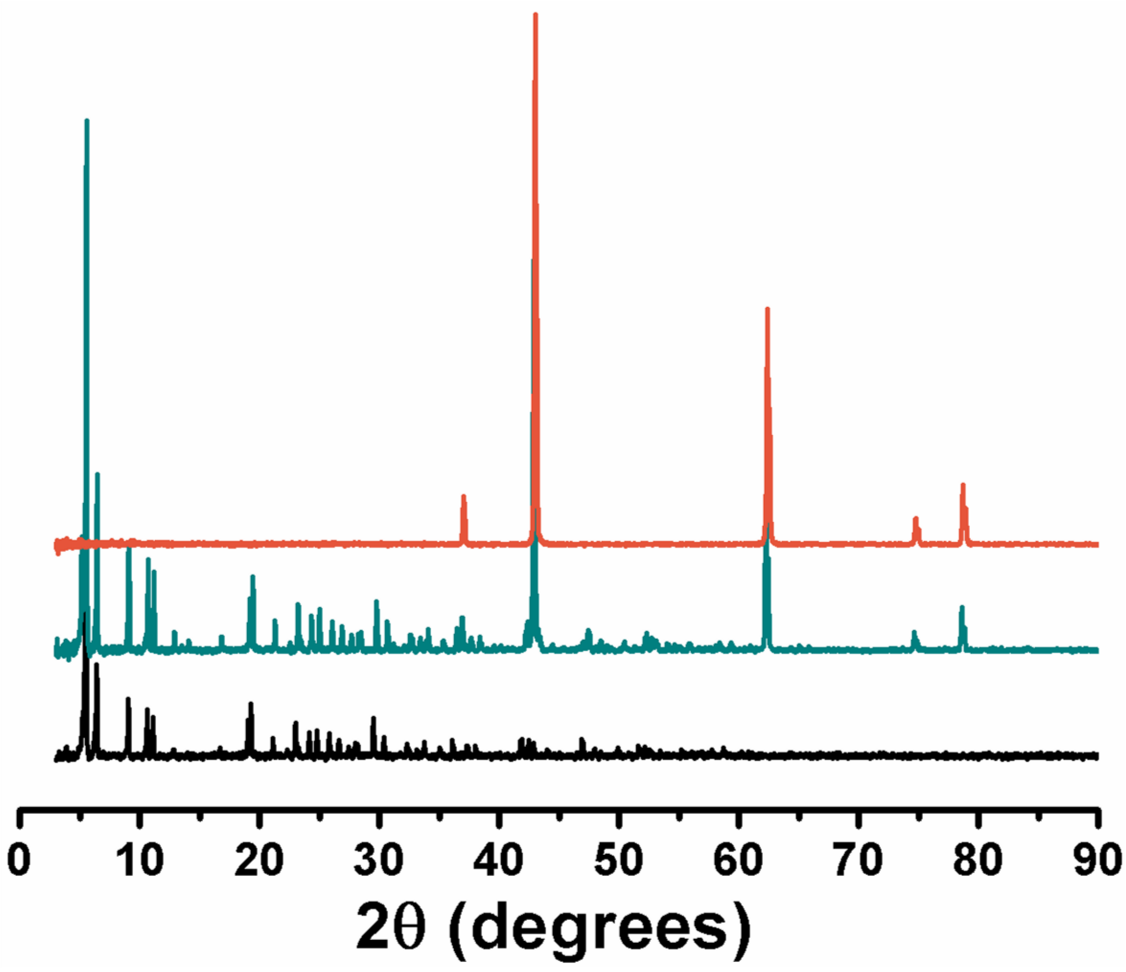

Fig. S33. PXRD comparing **dye@Yb^{3+}-BPDC** (black), **dye@Yb^{3+}-BPDC** + MgO (dark cyan), and MgO (orange).

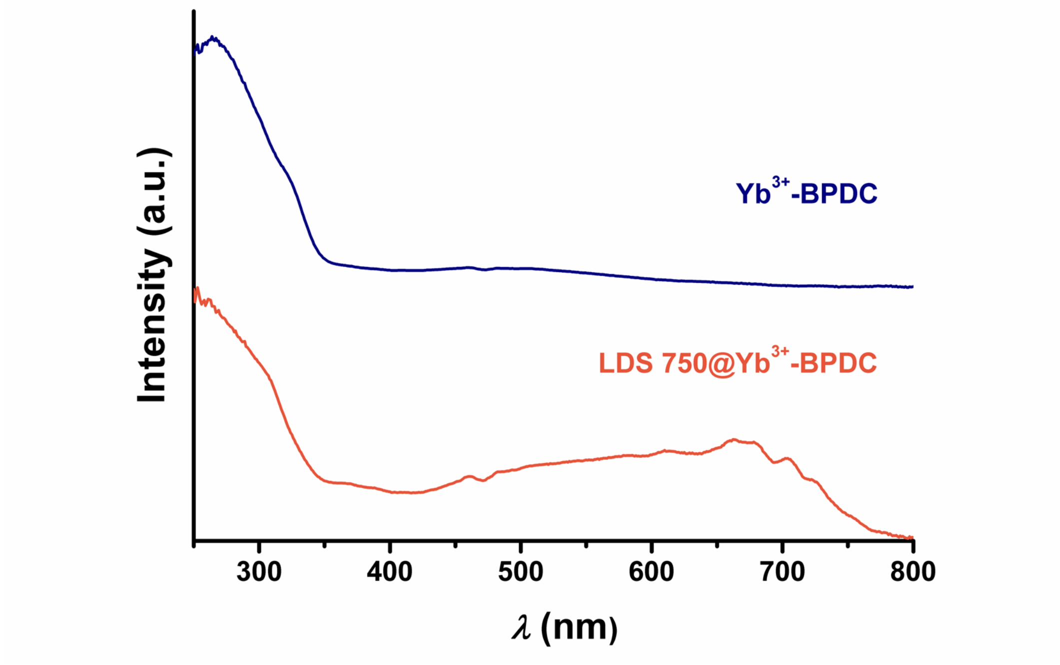

Fig. S34. Corrected and normalized excitation spectra upon monitoring emission at 980 nm of **Yb^{3+}-BPDC** (blue) and **LDS 750@Yb3+-BPDC** (red)

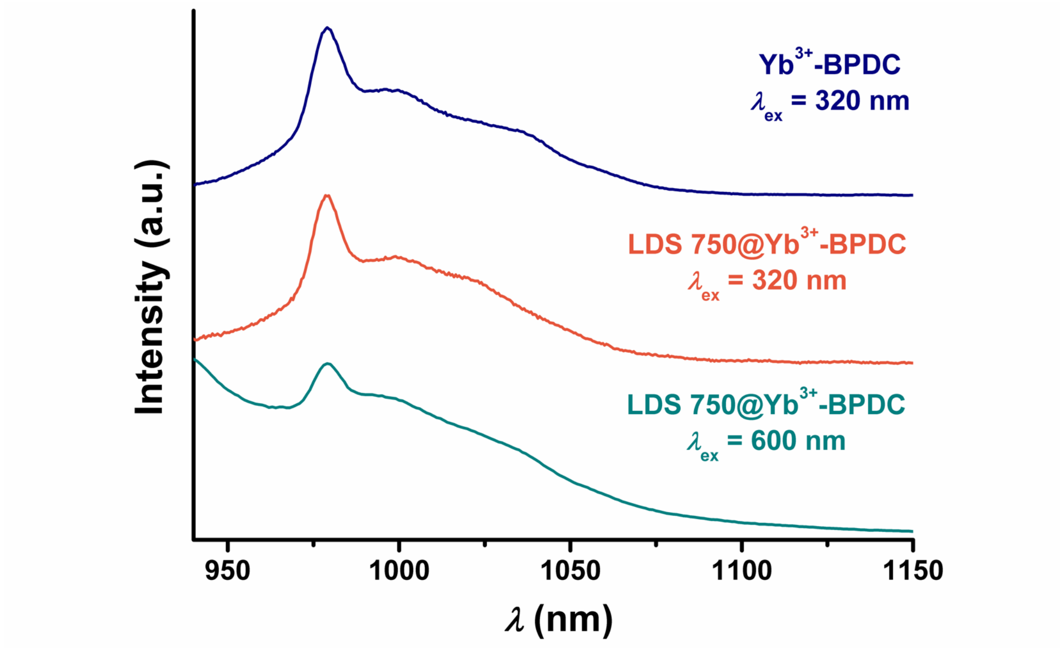

Fig. S35. Corrected and normalized emission spectra of **Yb^{3+}-BPDC** (excited at 320 nm, blue) and **LDS 750@Yb3+-BPDC** (excited at 320 nm, red; excited at 600 nm, dark cyan)

References:

1. G. Sheldrick, *Acta Crystallogr. A*, **2008**, *64*, 112-122.
2. G. Sheldrick, *Acta Crystallogr. C*, **2015**, *71*, 3-8.
3. O. V. Dolomanov, L. J. Bourhis, R. J. Gildea, J. A. K. Howard and H. Puschmann, *J. Appl. Crystallogr.*, **2009**, *42*, 339-341.
4. A. Spek, *Acta Crystallogr. D*, **2009**, *65*, 148-155.
5. V. Bon, I. Senkovska, M. S. Weiss and S. Kaskel, *CrystEngComm*, **2013**, *15*, 9572-9577.
6. C. F. Macrae, I. J. Bruno, J. A. Chisholm, P. R. Edgington, P. McCabe, E. Pidcock, L. Rodriguez-Monge, R. Taylor, J. van de Streek and P. A. Wood, *J. Appl. Crystallogr.*, **2008**, *41*, 466-470.
7. G. Sheldrick, *Acta Crystallogr. A*, **2015**, *71*, 3-8.